Reply to Referee Comment 1

We are very grateful to the reviewer for reading the manuscript extremely carefully and forwarding the valuable suggestions for improvement. Point-by-point responses to the reviewers' comments are listed below.

The reviewer's comment 1: The authors use MRI-CGCM3 data to estimate the future precipitation changes. Why do you choose MRI-CGCM3 data, not other Global Climate Models?

Authors' response: Thank you very much for the suggestions.

Compared to the other CGMs of CMIP5, the MRI-CGCM3 (Meteorological Research Institute Coupled Ocean-Atmosphere General Circulation Model3) performs better in simulating diurnal rainfall over subtropical China (Yuan et al. 2013) and has the finest resolution of 1.121° × 1.125°, thus being applied in Poyang Lake Watershed. And MRI-CGCM model is just a study case to examine the performance of STDDM. Other single-model is also ok to test the applicability of STDDM.

The references:

Yuan, W.: Diurnal cycles of precipitation over subtropical China in IPCC AR5 AMIP simulations, Adv. Atmos. Sci., 30(6), 1679–1694, doi:10.1007/s00376-013-2250-9, 2013.

The related content is in the manuscript in L114-120.

The reviewer's comment 2: The authors use precipitation simulations in RCP8.5 scenario from MRI-CGCMs to estimate precipitation changes under future climate warming. Why do you choose only RCP8.5 scenario, instead of other scenarios?

Authors' response: Thank you very much for the suggestions.

The future data includes simulations of the Representative Concentration Pathways (RCPs) of 8.5, 6.0, 4.5 and 2.6. Compared to the other RCPs, temperature increases the most in the RCP8.5 scenario, which corresponds to a highest greenhouse gas emission, leading to a radiative forcing of 8.5 W/m2 and temperature increment of 7.14 °C at the end of 21st century.

The research is to detect obvious changes of precipitations under climate warming. What we should do is

to display the significant change of precipitations in a scenario where temperature increment is large enough. Precipitation changes can be detected the most obviously under the climate warming scenario with temperature increasing the most. Compared to the other RCPs, the temperature in RCP8.5 scenario increased the most. So we select future simulations in the RCP8.5 scenario.

The related content is in L.121-125.

The reviewer's comment 3: The authors analyze the future precipitation changes in the Poyang Lake watershed using a Global Climate Model. The Poyang Lake watershed is a small area; while the Global Climate Model is coarse with resolution larger than 1 °x 1 °, which is difficult to be applied in a local scale such as the Poyang Lake watershed. The application could be reconsidered.

Authors' response: Thank you very much for the suggestions.

The Poyang Lake watershed is one of the major grain producing areas of China. In the south of the watershed, there is an internationally important habitat for migratory birds, abundant of biodiversity and regarded as Natural Reserve. The watershed is also a vital part of Yangtze River Economic Belt. However, floods and droughts occurs fluently in the Poyang Lake watershed, which cannot be immune to climate warming. As an important economic and ecological zones, what the precipitations changes in spatiotemporal distribution will be under the climate worming is a concern.

GCMs is a basic tool to analyze the future climate changes. As the resolution of GCMs is coarse unable to applied in small scale such as Poyang Lake Watershed, we downscaled the climate variables in the watershed with resolution of 20 km x 20 km. The uncertainty is $\leq$ 4.9%, demonstrating that the downscaled data can be applied in the Poyang Lake watershed.

The related content is in L68-76, L29-33 and L254-256 .

The reviewer's comment 4: In the methodology section, there is some confusions. What is the relationship between the STDDM and linear-scale algorithm? That should be explained more clearly.

Authors' response: Thank you very much for the suggestions.

STDDM is a logical frame, including three parts: upsampling GCMs simulations, constructing mapping relationships between the GCMs simulations and local observations, and correcting the GCMs

simulations. In the part 2 constructing relations, a transform function were built between the simulations and the local observations to transform simulations to no-bias data. The transform function could be any bias corrected model, including linear scaling, local intensity scaling, power transformation, distribution mapping models (Teutschbein et al. 2012) and so on. The transform model can be linear or no-linear regressions model. That is the relationship between the simulations and observations. In the study, the linear scaling algorithm was used as a transform function (also called as bias-corrected model), as a case study.

The references:

Teutschbein C, Seibert J. Bias correction of regional climate model simulations for hydrological climate-change impact studies: Review and evaluation of different methods [J]. Journal of Hydrology, 2012, 456: 12-29.

The revised paragraph of manuscript (Line 166-167):

Before the revises:

The bias correction was processed by using the translation function between match-ups of the up-sampled simulation and observation, which is the relations of the match-ups.

After the revises:

The bias correction was processed by the transform function between match-ups of the upsampled simulation and observations, which represents the mapping relationship between the match-ups. The transform function could be any bias corrected model, including linear scaling, local intensity scaling, power transformation, distribution mapping models (Teutschbein et al. 2012) and other linear or nonlinear regression models.

The reviewer's comment 5: By STDDM, you calculate the precipitation of each grid separately and get the downscaled precipitations. The downscaled precipitation is grid data. There may be some outstanding grid in which the precipitation is far different from the adjacent grids. According to first law of geography, near things are more related than distant things. So I suggest that the downscaled precipitation should be smoothed by smoothing filter.

Authors' response: Thank you very much for the suggestions.

The downscaled climate data is calculated based on the relationships between the up-sampled simulations and observations. The up-sampled simulations and observations are grid data. The relationships are the transform function between the match-ups of the simulation and observation. The transform function is constructed separately for match-ups in different grids. The grid data, including the simulations and observations, follows the first law of geography that the climate variable value is more related than distant grids. So the transform function based on the match-ups in nearer grids is more related than distant grids. Consequently, the climate variables calculated by the transform function should also follows the first low of geography. Besides, the downscaled results (precipitations in Fig. 9) shows almost no outstanding grid, which demonstrates that the results follows the first low of geography.

On the contrary, smoothing may lead to information missing of the climate variables.

So I think there could be no need to do smoothing.

The reviewer's comment 6: In 4.1 section, the validation period is from 1986 to 2005. However the observation data is from 1961 to 2005. Why not validate the downscaled precipitation in the same period from 1961 to 2005?

Authors' response: Thank you very much for the suggestions.

To avoid model overfitting, there should be calibrations and validations. In the study, the calibration and validation periods are from 1961 to 1985 and 1986 to 2005, separately. The downscaled model is constructed based on the data in calibration period. We should also need to know whether the model could be applied in the data of different time. So the validation period is different from the calibrations.

The model could be more correctly base on more data. So at last, we used all data from 1961 to 2005 to reconstruct the downscaling model.

The related content is in Line 170-172 and Line 227-230.

The reviewer's comment 7: Line199: The sentence missed a comma.

Authors' response: Thank you very much for the suggestions.

It has been revised in the manuscript.

The reviewer's comment 8: There are 69 references. Please provide the reference number for each reference. Is every reference useful to the research? If not, please delete some.

Authors' response: Thank you very much for the suggestions.

There is no need to add references number in the manuscript. All the references are useful to the study.

The reviewer's comment 9: Line197-200: Monthly precipitations, > 75% percentile of the 12 monthly precipitations, were classified as the extreme wet monthly precipitations for each year of the 103 years; monthly precipitations, ≤ 25% percentile were classified as the extreme dry monthly precipitation. The monthly precipitation of 25%-50% and 50%-75% quantiles are classified as normal dry and wet monthly precipitations. Why do the author classify the monthly precipitation into 4 categories, not 5 or 7? Why choose 25%, 50%, 50% and 75% quantiles as the classified boundary?

Authors' response: Thank you very much for the suggestions.

As the extreme wet and dry months cause floods and droughts more frequently, we pay more attention to the precipitations changes in extreme wet or dry months. So the months are differentiated as extreme and normal ones. The precipitation changes in wet and dry months also could show different condition, so the precipitation months in dry and wet should be separated. Here, we differentiate the months as the extreme wet, extreme dry, normal wet and normal dry ones. As for the classified boundary, it is more flexible. Several tries showed that 25%, 50%, 50% and 75% quantiles is appropriate classified standard. However, other classified standard is also OK, only if the precipitation changes of extreme wet, extreme dry, normal wet and normal dry months could be differentiated.

Reply to Referee Comment 2

We are very grateful to the reviewer for reading the manuscript extremely carefully and forwarding the valuable suggestions for improvement. Point-by-point responses to the reviewers' comments are listed below.

1. General comments

Reviewer's comment: However, the results, conclusions, and discussion presented in the current manuscript are not clear, concise, and well structured.

Authors' response: Thank you very much for the suggestion.

As you suggested, the results, conclusions, and discussion have been revised in the manuscript.

2. Specific Comments

Reviewer's comment 1: Assemble projection based on multi-GCMs has been widely used for regional future climate change scenarios, which is referred as the mainstream and popular method in the downscaling technique. However, only one GCM MRI-CGCM3 was selected in this study, based on the conclusions from Yuan et al. (2013) indicating a better performance in simulating diurnal rainfall over subtropical China, which is not enough for performance evaluation of multi-GCMs from CMIP5 in the specific Poyang Lake basin.

Authors' response: Thank you very much for the suggestion.

The research is mainly aimed to propose a spatiotemporal distributed downscaling method which could be applied to every single-GCM model. The MRI-CGCM3 is a study case to examine the model performance or availability of STDDM, as well as Poyang Lake which is taken as a study area. The validation is operated in several aspects. For the historical data, simulations from the GCM-downscaled result by STDDM and observations from meteorological stations were compared (Section 4.1). For the future data, we compared the future period (2081-2100) with the baseline period (1998-2017). The intra-annual and inner-annual variability were analyzed. The precipitation changes were also explained by climate warming in section 4.4. The explanation suggests the downscaling method is reasonable and STTDM could be applied in the basin-scale region based on a GCM successfully. The examination on a test GCM is necessary before STDDM could be used in other GCMs or multi-GCMs.

Indeed assemble projection is a mean stream. The model ensemble has a better model performance than the single-model assessed by R (correlation coefficient) and RMSE (Root-Mean-Square Error). However, the model ensemble is burdened with a smaller standard deviation (SD) than the single-models and observations (Fig 1). Except for R and RMSE, SD is also an important model evaluation index. The small SD value means small fluctuation, which demonstrates the fluctuation signal of original models (the signal-models) is not kept completely after being assembled. The SD of multi-GCMs is usually smaller

than original models (Fig 1). The monthly and daily variation are weakened in model ensembles. The ensemble can hardly analyze the seasonal or daily extreme event change exactly, taking the extreme dry (or wet) months and the max daily precipitation for example. In the study, we analyze the seasonal variations, as well as the change of extreme event intensities and frequencies. Using multi-GCMs can hardly reflect the application accuracy of STDDM precisely, in extreme climate analysis based on monthly and daily data. So a single-model should be selected to test the performance of STDDM.

A specific single-model could be used to analyze the seasonal change exactly, especially the extreme climate event change. As MRI-CGCM3 has the best spatial resolution among the CMIP5 GCMs, and a better performance in simulating diurnal rainfall over subtropical China, we took MRI-CGCM3 as a test case to apply in the Poyang Lake Basin and examine whether the STDDM can be used to produce reasonable monthly and daily data, especially the extreme climate change.

The title *Variations of future precipitations in Poyang Lake Watershed under global warming using a spatiotemporally distributed downscaling model* might confuse you. So it will be revised as *Precipitation projection using a spatiotemporal distributed method: a case study in Poyang Lake Basin based on MRI-CGCM3*. And the content will be revised corresponding to the revised title.

In summary, using multi-GCMs instead of MRI-CGCM3 in the study could be reconsidered.

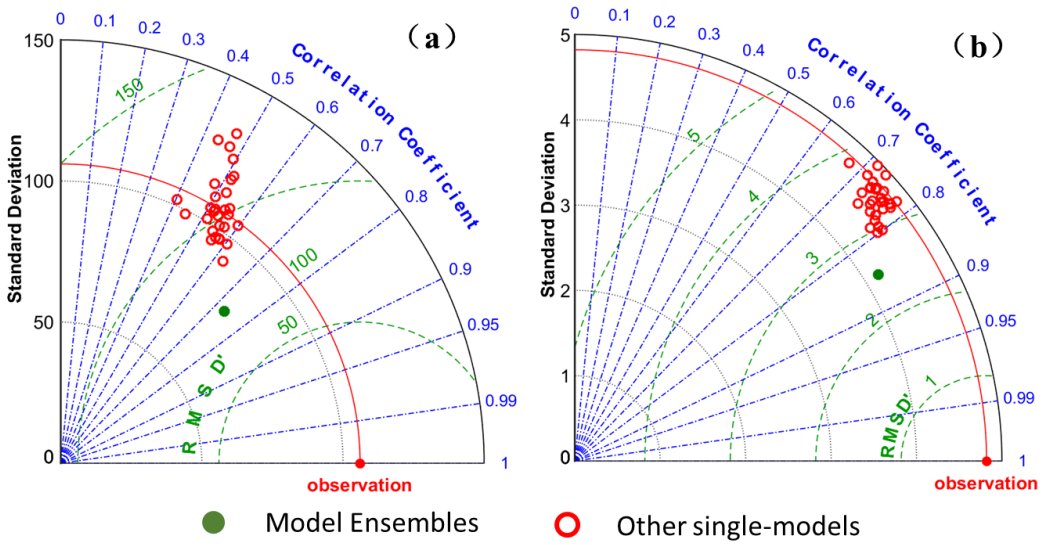

Figure 1. The Taylor figures (Taylor et al.,2001) of model evaluation. Following Taylor et al. (2001), the radial distance from the origin denotes the standard deviation of each data set (the primary observations are shown as a red line) and the angular distance from the horizontal denotes the correlation coefficient r between each model data set and the primary observations. The centered RMS error (RMSE') is indicated by the distance to the intersection of the green dashed line and the horizontal axis with units and magnitude indicated by the radial axis. The model ensemble is constructed by a genetic algorithm. The genetic algorithm is used to calculate the best weigh for each single-model, assuming RMSE' as the cost function. The model ensemble is the weighted sum of each single-model. The other single-models include ACCESS1-0, ACCESS1-3, BCC-CSM1-1-m, BCC-CSM1-1, BNU-ESM, CanESM2, CCSM4, CMCC-

CMS, CMCC-CM, CNRM-CM5, FGOALS-g2, GISS-E2-H-CC, GISS-E2-H, GISS-E2-R-CC, GISS-E2-R, HadGEM2-AO, HadGEM2-CC, HadGEM2-ES, inmcm4, IPSL-CM5A-LR, IPSL-CM5A-MR, IPSL-CM5B-LR, MIROC-ESM-CHEM, MIROC-ESM, MIROC5, MPI-ESM-LR, MPI-ESM-MR, MRI-CGCM3 and NorESM1-M. The model description can be obtained from *https://pcmdi.llnl.gov/mips/cmip5/availability.html*.

The references:

Taylor K E. Summarizing multiple aspects of model performance in a single diagram [J]. Journal of Geophysical Research: Atmospheres, 2001, 106(D7): 7183-7192.

The main revised paragraph of manuscript (Line 1-2):

Before the revises:

Variations of future precipitations in Poyang Lake Watershed under the global warming using a spatiotemporally distributed downscaling model

After the revises:

Precipitation projections using a spatiotemporal distributed method: a case study in the Poyang Lake Watershed based on MRI-CGCM3

Reviewer's comment 2: In order to detect the sensitivity of precipitation change under global climate warming, different RCP scenarios should be selected to do comparative analysis. However, only RCP 8.5 was selected to generate future climate change scenarios in the current manuscript, which is insufficient to obtain a scientific and convinced projection for the study area.

Authors' response: Thank you very much for the suggestion.

The future data includes simulations of the Representative Concentration Pathways (RCPs) of 8.5, 6.0, 4.5 and 2.6. Compared to the other RCPs, temperature increases the most in the RCP8.5 scenario, which corresponds to a highest greenhouse gas emission, leading to a radiative forcing of 8.5 W/m2 and temperature increase of 7.14 °C at the end of 21st century.

The research is to detect remarkable precipitation changes under climate warming, which should be pronounced enough to be acknowledged by us. To get the obvious precipitation changes, what we should do is to obtain the future precipitation in a high-emission scenario where the temperature increment is large enough. Compared to the other RCPs, the temperature increment in RCP8.5 scenario is the largest. So we select future simulations in the RCP8.5 scenario.

Although it is valuable to detect the sensitivity of precipitation change, the sensitivity analysis is not the purpose of the study. And there are many climate change related researches (Gourdji et al.,2013; Sillmann et al.,2013; De et al., 2014; Cai et al.,2017) only use the high-emissions scenario to investigate the impacts of climate warming. The result from RCP8.5 scenario is the most remarkable, from which we can get the obvious change and know what will happen when climate warming gets worse. The study is to investigate the remarkable change of precipitation under climate warming.

So it could be reasonable to only select RCP85 scenario in the experiment to detect the significant changes of precipitation.

The references:

De Lavergne C, Palter J B, Galbraith E D, et al. Cessation of deep convection in the open Southern Ocean under anthropogenic climate change [J]. Nature Climate Change, 2014, 4(4): 278.

Cai W, Li K, Liao H, et al. Weather conditions conducive to Beijing severe haze more frequent under climate change[J]. Nature Climate Change, 2017, 7(4): 257.

Gourdji, S. M., Sibley, A. M. & Lobell, D. B. Global crop exposure to critical high temperatures in the reproductive period: Historical trends and future projections. Environ. Res. Lett. 8, 024041 (2013).

Sillmann J, Kharin V V, Zwiers F W, et al. Climate extremes indices in the CMIP5 multi-model ensemble: Part 2. Future climate projections[J]. Journal of Geophysical Research: Atmospheres, 2013, 118(6): 2473-2493.

The main revised in the manuscript (Line 122-123):

Before the revises:

Thus, to detect more sensitive precipitation change under climate warming, we selected future simulations in the RCP8.5 scenario.

After the revises:

The research is to detect the remarkable precipitation changes under climate warming; thus we selected future simulations in the RCP8.5 scenario.

Reviewer's comment 3: Too many time periods are defined in the manuscript corresponding to different years, such as baseline and future periods, historical, historical extent and future, etc., which would make readers confused and difficult to understand.

Authors' response: Thank you very much for the suggestion.

Cmip5 GCMs include historical (1850-2005), historical extent (2006-2012), RCPs (2005-2100 or 2005-2300) scenarios (Friedlingstein et al., 2008). At the WGCM meeting in October 2011, there was agreement that it would be useful to extend the CMIP5 historical runs to near-present 2012, rather than ending them in 2005 (Friedlingstein et al., 2008). So another scenario (historical extension) from 2006 to 2012 was constructed to extend the historical data to 2012. In the study, we merge the historical (from 1961 to 2005), historical extent (from 2006 to 2012) and RCP85 (from 2013 to 2100) data, as merged data (1961-2100). From the merged data, simulations from 1998 to 2017 were selected as the baseline period data, and simulations from 2081 to 2100 were selected as the future period data.

The references:

Friedlingstein OB, Webb M, Gregory J. A Summary of the CMIP5 Experiment Design [J]. 2008.

The main revised paragraph of manuscript (Line 117-134):

Before the revises:

From MRI-CGCM3, we select historical (1961 to 2005), historical extent (2006 to 2012) and future (2006 to 2100) precipitation and temperature simulations. The future data includes simulations of the Representative Concentration Pathways (RCPs) of 8.5,6, 4.5 and 2.6. Compared to the other RCPs, in the RCP8.5 scenario temperature increases the most, which is corresponds to a highest greenhouse gas emission, leading to a radiative forcing of 8.5 W/m2 and temperature increase of 7.14 °C at the end of 21st century (Taylor et al. 2012). Thus, to detect more sensitive precipitation change under climate warming, we selected future simulations in the RCP8.5 scenario.

The local grid observations (Zhao et al., 2014) with a resolution of 0.5°×0.5° are downloaded from the China Meteorological Data Service Center (http://data.cma.cn/). The local grid observations and MRI-CGCM3 historical simulations were used to construct relationship to correct the MRI-CGCM3 data. China metrology point data were also downscaled and used to validate the bias-corrected MRI-CGCM3 simulations. To investigate the relationship between precipitation changes and the temperature increase, we extract not only temperature data, but also precipitations.

To quantitatively analyse the precipitation changes under climate warming in 21st century, we compared precipitation between the baseline and future period. As annual precipitation observations have main oscillation periods of quasi-20 years (Zhan et al. 2011), we selected three 20 years, the baseline period from 1998 to 2017, the near future period from 2041 to 2060 and the far future period from 2081 to 2100. We merge historical simulations from 1998 to 2005, and historical extent simulations from 2006 to 2012, and RCP8.5 simulations from 2013 to 2017, which is the nearest 20 years and thus selected as the baseline period. The data in near and far future period are derived from simulations in RCP8.5 scenarios.

After the revises:

Thus we select MRI-CGCM3 data applied in Poyang Lake Watershed to test the performance of the STDDM.

The future data of MRI-CGCM3 includes simulations of the Representative Concentration Pathways (RCPs) of 8.5,6, 4.5 and 2.6. Compared to the other RCPs, in the RCP8.5 scenario temperature increases the most, which is corresponds to a highest greenhouse gas emission, leading to a radiative forcing of 8.5 W/m2 and temperature increase of 7.14 °C at the end of 21st century (Taylor et al. 2012). The research is to detect the remarkable precipitation changes under climate warming; thus we selected future simulations in the RCP8.5 scenario. In the study, we merge the historical (from 1961 to 2005), historical extent (from 2006 to 2012) and RCP85 (from 2013 to 2100) data, as the merged data (1961-2100). To quantitatively analyze the precipitation changes under climate warming in 21st century, we compared precipitation between the baseline and future period. As annual precipitation observations have main oscillation periods of quasi-20 years (Zhan et al. 2011), we selected three 20 years from the merged data. From the merged data, simulations from 1998 to 2017 were selected as the baseline period data, simulations from 2041 to

2060 were selected as the near future period data, and simulations from 2081 to 2100 were selected as the further future period data.

The local grid observations (Zhao et al., 2014) with a resolution of 0.5°×0.5° are downloaded from the China Meteorological Data Service Center (http://data.cma.cn/). The local grid observations and MRI-CGCM3 historical simulations were used to construct relationship to correct the GCM data. China metrology point data were also downscaled and used to validate the grid observations and the downscaled GCM simulations. To investigate the relationship between precipitation changes and the temperature increment, we extract not only precipitations, but also temperature.

Reviewer's comment 4: It will be better to add an evaluation section for the gridded meteorological data by using gauging stations observation.

Authors' response: Thank you very much for the suggestion.

The evaluation for the gridded meteorological data has be added in the manuscript.

The following was added in the manuscript (Line 238-239):

Validation about the China meteorological grid observations should be performed, as well as the STDDM. As the STDDM introduce the China meteorological grid observations and the grid data is not the direct in-suit data, validation about the gridded data is necessary. The determination coefficient (R2), root mean square error (RMSE) and PBias (percent bias) were used to examine the model performance.

The following was added after Line 570:

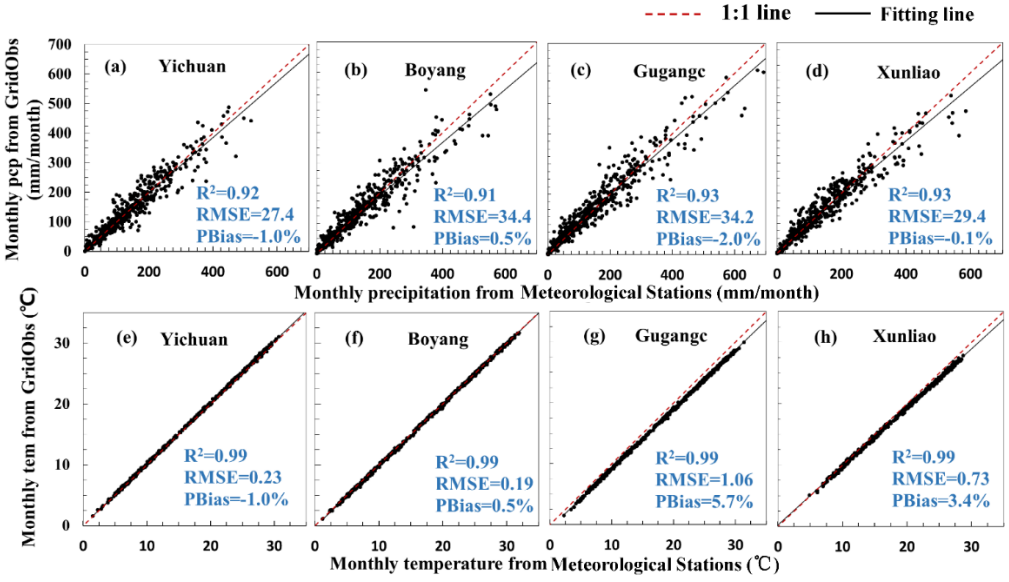

Fig. 3. Validation of gridded meteorological data (GridObs) by using gauging stations observation: Precipitation (pcp; a,b,c and d) and temperature (tem; e,d,f and g) at meteorological station of Jian (a and e), Ganzhou (b and d), Zhangshu (c and f) and Lushan (d and g).

Reviewer's comment 5: English writing is poor in the current manuscript, which needs to be polished

by a native English-speaking editor. Examples of grammar errors are as follows:

Line 27: threating to → threatening

Line 37: constructed → constructs

Line 43: in the station scale → at the station scale, many similar errors in other paragraphs.

Line 45: as underlays of the local region is complex → as underlays of local region are complex

Line 57: project → projects

Line 69: Precipitation redistributions under global warming has → Precipitation redistributions under global warming have

Line 77: includes → include

Line 84: metrological → meteorological, many similar errors in other sentences. Figure 2, 1(a): observitions → observations

Authors' response: Thank you very much for the language editing.

The writing errors has been revised in the manuscript.

~~Variations of future precipitations~~Precipitation projections using a spatiotemporal distributed method: a case study in the Poyang Lake Watershed ~~under the global warming using a spatiotemporally distributed downscaling model~~based on MRI-CGCM3

Ling Zhang [1], Xiaoling Chen[1, 2], Jianzhong Lu[1, *], Dong Liang[1]

[1]State Key Laboratory of Information Engineering in Surveying, Mapping and Remote Sensing, Wuhan University, Wuhan 430079, China

[2]Key Laboratory of Poyang Lake Wetland and Watershed Research, Ministry of Education, Jiangxi Normal University, Nanchang 330022, China

* *Correspondence to*: Jianzhong Lu (lujzhong@whu.edu.cn)

Abstract. Traditional ~~statistic~~statistical downscaling methods are ~~processed~~performed on independent ~~stations, which ignores~~station measurements and ignore spatial correlations and spatiotemporal heterogeneity. In this study, a spatiotemporally distributed downscaling model (STDDM) was developed. ~~The~~Using this method, we interpolated grid observations and ~~GCMs~~GCM (Global Climate ~~Models~~Model) simulations to ~~continual~~continuously finer grids~~;~~ and then created mapping relationship between the observations and the simulations, respectively for each grid at each time. We applied the STDDM ~~in~~to precipitation downscaling ~~of~~in Poyang Lake Watershed using MRI-CGCM3 (Meteorological Research Institute Coupled Ocean-Atmosphere General Circulation Model3), with an ~~acceptant~~accepted uncertainty of ⩽ 4.9~~%, and~~%; then created future precipitation changes from 1998 to 2100 (1998-2012 in the historical and 2013-2100 in the RCP8.5 scenario). The precipitation changes ~~showed increasing~~ increased heterogeneities in temporal and spatial distribution under ~~the~~ future climate warming. In ~~the~~terms of temporal ~~pattern~~patterns, the wet season ~~precipitation increased with change rate (CR) = 7.33 mm/10a (11.66 mm/K)~~ become wetter while the dry season ~~precipitations decreased with CR = −0.92 mm/10a (−4.31 mm/K).~~become drier. The frequency of extreme precipitation ~~frequency and intensity were enhanced with CR=0.49~~increased while that of the moderate precipitation decreased. Total precipitation increased while rain days~~/10a and 7.2mm•day^{-1}/10a respectively. In~~ decreased. The max continuous dry days and the max daily precipitation both increased. In terms of spatial ~~pattern, precipitations in wet or dry season showed an uneven change rate over~~patterns, the ~~watershed, and the wet or~~ dry area exhibited a ~~wetter or~~ drier condition ~~in~~during the ~~wet or~~ dry season; the wet area exhibited a wetter condition during the wet season. Analysis with temperature ~~increases~~increment showed precipitation changes ~~appeared~~can be significantly ~~(~~explained by climate warming, with $p < 0.05$ and $R \geqslant 0.56$~~) correlated to climate warming~~. The precipitation changes and explains indicated the downscaling method is reasonable and the STDDM could be applied in the basin-scale region based on a GCM successfully. The results implicated ~~the~~an increasing risk of flood-droughts under global warming ~~and~~, which were a reference for water balance analysis and water resource planting.

1 Introduction

Global warming has caused ~~precipitation redistribution in~~ temporal and spatial ~~distribution~~ redistributions of precipitation (Frei et al. 1998; Trenberth et al. 2011~~), increasing~~) and has increased the frequency and intensity of floods and droughts, ~~thus~~ seriously threating ~~to~~ social systems and ecosystems (Pall et al, 2000; Dai, 2013). To the fragile ecological and living ~~environment~~environments, what the future hydrological situation will be under future global warming is a crucial question to avoid or reduce damages from climate warming.

~~As a~~Global Climate Models (GCMs) are basic ~~tool in~~tools for assessing the effects of future climate change ~~effects, Global Climate Models (GCMs)~~ and provide an initial source ~~of~~for future climates (Xu, 1999). However, GCMs ~~remain~~have coarse ~~with~~ global resolutions ~~larger than~~ranging from 1°×1°~~, which is unable~~ to ~~apply~~4°×4°, and are not applicable in regional ~~scale~~scales, such as watersheds. Downscaling algorithms have been developed to link the global-scale GCMs outputs and the regional-scale climate variables, including dynamic (Giorgi, 1990; Teutschbein and Seibert, 2012) and statistic (Wilby et al., 2007; Chu et al., 2010) models. The dynamic method employs regional climate models (RCMs) that are nested inside GCMs based on the complex physics of atmospheric processes and involves high computational costs. Limited by an insufficient understanding of the physical mechanism and expensively computing resources, the dynamic downscaling model cannot easily satisfy small and mid-size region as the Poyang Lake ~~Basin~~Watershed. Unlike dynamic downscaling ~~models~~, statistic downscaling ~~constructed~~constructs an empirical relationship between climate variables of the global-scale ~~output~~ and local-scale ~~climate variables~~, with inexpensive computations. ~~Benefitting~~Benefiting from inexpensive computations and easy implementations, downscaling methods have been widely used, including regression models (Labraga et al. 2010, Quintana et al. 2010; Zorita et al. 1999), weather typing schemes (Boéj et al. 2007; ENKE et al. 2005) and weather generators (Mullan et al., 2016; Baigorria and Jones et al., 2011).

In these ~~researchess~~studies, statistical downscaling methods have been developed based on the relationship between the global-scale simulations and the local station-scale observations ~~in the station scale.~~. The methods are ~~processed~~conducted on each station, independently. Thus, the specific downscaling relationship and downscaled climate variable~~,~~ are both independent and discrete ~~in~~at the station scale, instead of being spatially continuous ~~in grid scale with~~at a ~~finer~~ fine-resolution grid-scale. However, as underlays of local region ~~is~~are complex with different topographies, land covers, and clouds coverage, the downscaling relationships and downscaled climate variables at discrete stations ~~can't~~cannot clearly express the spatial heterogeneity ~~clearly~~, compared to the spatially continuous data. ~~Particularly, for the~~ For ungauged ~~area~~areas without ~~stations covered~~station coverage, it is inviable to ~~get~~obtain high-quality ~~of~~ downscaling relationships and downscaled local ~~climates~~climate variables. Moreover, the downscaled local climate results and downscaling ~~relationship in~~relationships at the station scale~~,~~ are difficult to show the spatial correlation; ~~whereas~~however, results from the downscaling ~~which is~~, processed on spatially continuous data, such as finer grids, can naturally show spatial ~~relationship naturally:~~relationships. Additionally, spatially continuous data can be directly used in ~~the~~a spatially distributed hydrological model, such as Crest (Wang et al., 2011), VIC (Lohmann et al. 1998), and MIKE SHE (DHI, 2014), which is the ~~focus and frontier~~forefront of international hydrological scientific research (Beven et al. 1990). ~~Besides,~~ In addition, spatially continuous downscaled climate data ~~in spatially continuous pattern~~ can be easily integrated with remote sensing data of geologies, topographies, soils, or land covers. In fact, spatially continuous data is widely used ~~as~~ in the rapidly developing field of remote sensing ~~technology develops rapidly~~, which benefits hydrological models by providing a data source (Engman et al., 1991). Therefore, the downscaling method processed on spatially continuous data is of vital importance. ~~The spatial distributed~~ For the continuous space covered with complex underlays, statistical downscaling ~~method, which creates~~methods should take spatial heterogeneity into consideration, thus creating downscaling ~~relationship and project climates~~ relationships spatially distributed at ~~spatial~~spatially continuous scale~~, should be taken into consideration.~~.

In addition to ~~the~~ spatial heterogeneity, the relationship between the climate variables ~~of~~at the global-scale and local-scale also shows ~~different in~~ temporal heterogeneity ~~of one~~in a single year, ~~as dominator affecting~~because the dominators that affect climate ~~varies in different~~ vary through time (~~eg.~~e.g., seasons or ~~Months~~months).

Therefore, ~~the temporal~~a temporally distributed downscaling method, which creates different ~~relationship~~relationships at different ~~time~~times, should be taken into consideration. However, many downscaling methods ~~didn't take~~have not taken temporal heterogeneity into consideration. For each ~~individual~~ observed site, the established downscaling method was a global standard for the whole time ~~series data~~, instead of being different in separate seasons or ~~Months~~months (Labraga 2010; Wu et al., 2017; Sachindra et al., 2018). In the study, ~~the~~ temporally distributed downscaling ~~could be~~is considered. Combining ~~the~~temporal heterogeneity and spatial heterogeneity in ~~time and~~ continual space, a climate downscaling model based on ~~spatiotemporal~~a spatiotemporally distributed framework~~, a spatiotemporal~~ (a spatiotemporally distributed downscaling method~~,~~), should be proposed to project future climate ~~changes in~~at a regional scale.

~~Sensitive~~The Poyang Lake Watershed is sensitive to climate changes in the East Asian monsoon region~~, Poyang Lake Watershed~~ and therefore is not immune to global warming. ~~Precipitation redistributions under~~ Redistributions of precipitation due to global warming ~~has caused more~~ have resulted in an increased occurrence of extreme hydrological events, ~~with manifestation of the~~an enhanced flood frequency and intensity (Wang et al., 2009; Guo et al., 2006), a significant decline ~~of~~in lake level and inundation area (Feng et al. 2012; Zhang et al. 2014), which ~~poses a threat~~threatened to ~~the~~ fragile wetland and forest ~~ecosystem~~ecosystems (Han et al. 2015, Dyderski et al. 2018), economic developments and ~~people's~~human lives (Ye et al., 2011).

However, the Poyang Lake Wetland ecosystem~~,~~ is an internationally important habitat for migratory birds, abundant of biodiversity and regarded as a Natural Reserve~~:~~. In addition, the watershed is a commercial grain production area~~,~~ and an important part of the Yangtze River Economic Belt. As ~~a~~ this region is economically and ecologically significant ~~economic and ecosystem region~~, investigating the future precipitation changes in the watershed is ~~crutial~~crucial for ~~prevention~~protection from climate damages. Previous studies of future precipitation changes in the Poyang Lake Watershed ~~includes~~include temporal and special ~~pattern~~patterns. Precipitation changes in temporal pattern, focused on intensity and frequency of precipitation extremes (Hong et al. 2014; Wang et al. 2017), as well as the annual or quarterly total ~~precipitations~~precipitation (Guo et al., 2010; Guo et al., 2008; Li et al., 2016). In spatial pattern, precipitation change analysis ~~is based on the~~ covers five ~~sub-basins~~subbasins (Xinjiang, Raohe, Xiushui, Ganjiang and Fuhe ~~sub-basins~~subbasins) (Guo, et al. 2010; Hong, et al. 2014~~),~~) and 13 discrete ~~metrological~~meteorological stations (Li et al. 2016), or 7 coarse grids (Guo, et al. 2008). ~~Little~~There has been little research ~~concerns on~~ concerning the spatial-temporal distribution ~~with~~of precipitation in a continual ~~finer~~fine-resolution grids space~~, not to mention the possible~~. In addition, a driving force analysis ~~for~~of precipitation changes related to ~~increasing~~ temperatures increment has not been conducted.

In the study, taking Poyang Lake Watershed as a test case, we projected future precipitations based on the ~~spatiotemporal~~spatiotemporally distributed downscaling method (STDDM), using MRI-GCM3 simulations and ~~metrological~~meteorological observations~~, with~~. The objects are as the following ~~specific objects~~: (1) ~~developing~~to develop a ~~spatiotemporal~~spatiotemporally distributed downscaling method (STDDM~~) for spatially continual~~), projecting future climate variables ~~projections; in~~ spatially continual scale; and (2) ~~documenting precipitation changes in~~ to document temporal and spatial ~~pattern~~changes in precipitation for the Poyang Lake Watershed in the ~~21th~~21st century~~,~~ and the correlations between these precipitation changes and temperature ~~increasing~~increment. Future precipitation changes can provide basic hydrological information necessary to ~~get~~ a better understanding of water ~~resource~~ volumes and flood-droughts risks~~, which~~; furtherly benefits ~~a scientific sight in~~ wetland and forest ecosystem conservation~~,~~ and aids decision--making in development, utilization, and planning of water resources.

2 Study area and datasets

2.1 Study Area

Poyang Lake Basin (24°28'-30°05' N and 113°33'-118°29'E) is located in the southeast of China, connected with Yangtze River in the north (Fig. 1). Within the southeast subtropical monsoon zone, the annual average temperature of the watershed is 17.5C°. The mean annual precipitation is ~~1638mm~~1638 mm, with 192 rainy days (daily precipitation ≥ 0.1 mm/day) and 173 rain-free days (daily precipitation < 0.1 mm/day). The rainy season

lasts from April to July, occupying about 70% of the annual total amount. Inter or intra annual precipitation variations are dominated by the southeast and southwest monsoon, mainly in summer. With a coverage area of 162000 km^2, the diversities of topographies also ~~affect~~effect on precipitation changes. The topography varies from high mountains of Luoxiao, Wuyi, and Nanling in east, south and west, with the elevation reaching to the 2200m, to the depressing of Ji Tai or Ganzhou Depressing in the south or center and alluvial plains of Poyang Lake Plain in the north, with the elevation reaching to <50 m (~~Fig.~~ 1a). The different topography and location generate the uneven distribution ~~rain~~ of precipitation in space~~, with~~ and produce less rain in the depressing, plains, and hills area ~~for~~because of the leeward sloop, but more orographic rain in the mountain area ~~because~~for the reason of the windward sloop (~~Fig.~~ 1b) (Mingjin et al. 2011). To ~~analyse~~analyze precipitation changes in the rich- or ~~-~~poor-rain area, the ~~metrological~~meteorological stations were classified into dry and wet stations (Fig. 1a and b), according to the annual precipitation amount. We sorted the annual precipitation averaged over the time from 1961 to 2005, of the 15 stations. The ~~4~~four stations with the max or min mean annual precipitations are set as dry or wet stations, indicating the dry or wet area~~,~~ (Fig.1b), respectively.

In the past 50 years of the Poyang Lake Watershed, annual mean temperature indeed experiences a significant ($p<0.02$) increase with a change rate of 0.15 C°/10a (Fig.1d), based on the ~~metrological~~meteorological observations from 1961 to 2005. Under the temperature increasing condition, the precipitation in temporal and spatial distribution becomes more uneven (Zhan et al. 2011), which increases the risk of floods and droughts (Li et al. 2016; Ye et al. 2011).

2.2 Data sets

Global Climate Models (GCMs) are widely used tools to project future climate change. GCMs from the Coupled Model Intercomparison Project Phase Five (CMIP5) performs better than other CMIPs such as CMIP3 and CMIP4, with generally finer resolution and more improved physical mechanism (Sperber, 2013; Taylor et al. 2012). Compared to the other CGMs of CMIP5, the MRI-CGCM3 (Meteorological Research Institute Coupled Ocean-Atmosphere General Circulation Model3, Yukimoto et al. 2012) performs better in simulating diurnal rainfall over subtropical China (Yuan et al. 2013) and has the finest resolution of 1.121° × 1.125°~~, thus being~~. Thus we select MRI-CGCM3 data applied in Poyang Lake Watershed~~. From MRI-CGCM3, we select historical (1961~~ to ~~2005), historical extent (2006 to 2012) and future (2006 to 2100) precipitation and temperature simulations.~~ test the performance of the STDDM.

The future data of MRI-CGCM3 includes simulations of the Representative Concentration Pathways (RCPs) of 8.5,6, 4.5 and 2.6. Compared to the other RCPs, in the RCP8.5 scenario temperature increases the most, which is corresponds to a highest greenhouse gas emission, leading to a radiative forcing of 8.5 W/m^2 and temperature increase of 7.14 °C at the end of 21st century (Taylor et al. 2012). The research is to detect the remarkable precipitation changes under climate warming; thus we selected future simulations in the RCP8.5 scenario. In the study, we merge the historical (from 1961 to 2005), historical extent (from 2006 to 2012) and RCP85 (from 2013 to 2100) data, as the merged data (1961-2100). To quantitatively analyze the precipitation changes under climate warming in the 21st century, we compared precipitation between the baseline and future period. As annual precipitation observations have main oscillation periods of quasi-20 years (Zhan et al. ~~2012). Thus, to detect more sensitive precipitation change under climate warming, we selected future simulations in the RCP8.5 scenario.~~ 2011), we selected three 20 years from the merged data. From the merged data, simulations from 1998 to 2017 were selected as the baseline period data, simulations from 2041 to 2060 were selected as the near future period data, and simulations from 2081 to 2100 were selected as the further future period data.

The local grid observations (Zhao et al., 2014) with a resolution of 0.5°×0.5° are downloaded from the China Meteorological Data Service Center (http://data.cma.cn/). The local grid observations and MRI-CGCM3 historical simulations were used to construct a relationship to correct the ~~MRI-CGCM3~~GCM data. China metrology point data were also downscaled and used to validate the ~~bias-corrected MRI-CGCM3~~grid observations and the downscaled GCM simulations. To investigate the relationship between precipitation changes and the temperature ~~increase~~increment, we extract not only ~~temperature data, but also~~ precipitations but also temperature.

~~To quantitatively analyse the precipitation changes under climate warming in 21st century, we compared~~

precipitation between the baseline and future period. As annual precipitation observations have main oscillation periods of quasi-20 years (Zhan et al. 2011), we selected three 20 years, the baseline period from 1998 to 2017, the near future period from 2041 to 2060 and the far future period from 2081 to 2100. We merge historical simulations from 1998 to 2005, and historical extent simulations from 2006 to 2012, and RCP8.5 simulations from 2013 to 2017, which is the nearest 20 years and thus selected as the baseline period. The data in near and far future period are derived from simulations in RCP8.5 scenarios.

3 Methodology

3.1 Future climatesclimate projection based on the spatiotemporally distributed downscaling model

Considering the spatiotemporal heterogeneity of precipitations inprecipitation at the regional scale such as the Poyang Lake Watershed, we developed a spatiotemporally distributed downscaling model (STDDM), which is a logical framework based on a specific mathematic algorithm. The mathematic algorithm was used to create a mapping relationship between GCMsthe global-scale GCM simulations in the global scale and the local scale climates variables in the local scale.. The mapping relationship is used as a translationtransform function to translatecorrect the future climate simulations from the GCMs scale to regional scale.no-bias data. In the framework, we constructed respective mapping relationships between the corresponding matchematch-ups of GCMs simulations and local climate observations in each different time (eg. Monthse.g., months or seasons) at each different location, were constructed.. The STDDM was improved incompared to the traditional downscaling methods by adjusting the specific downscaling algorithm to be suitable to in the distributed space and time, where. Therefore, the downscaling process shows spatiotemporally differentprocesses show spatiotemporal differences in the parameters or the equations, and the output data are spatial continued, compared to thespatially continuous, unlike that in traditional downscaling methods, which ignores the temporal and continuouslycontinuous spatial difference in the downscaling processdifferences and expresses the express space byas discrete points instead of continual space andcontinuous grids.

Figure 2a shows the logical framework of the STDDM while Fig. 2b demonstrates how it was applied in Poyang Lake Watershed using MRI-CGCM3 based on a linear-scaling algorithm. The STDDM contains three parts (Fig. 2a and b): (1) Up-samplingupsampling GCMs simulations and local-scale observations to a continualcontinuous grid space of the same finer resolution; (2) Constructingconstructing respective mapping relationship between the GCMs simulations and local observations in distributed space and time; (3) Correctingcorrecting the GCMs simulations of the future scenario, using the relationsmapping relationship constructed in step 2.

3.1.1 Up-samplingUpsampling GCMs simulations

With a coarse resolution, unable to be integrated with sub-grid scale features (Grotch and Maccracken,1991) such as topography and land use, the GCMs simulations should be up-sampled to a finer resolution. To get corresponding match-ups of the global scale simulation and local scale observation in respective time and space, we up-sampled both GCMs simulations and observations into the same spatial continual grid with a high resolution (Fig. 2a).

In the study, MRI-GCM3 simulations were interpolated by Natural NeighbourNeighbor Interpolation (Sibson et al., 1981),) to a scale of 20 km×20 km, the smallest size of the sub-basinsubbasin of the Poyang Lake Watershed (Zhang et al. 2017), generating 263 spatial grids (Fig. 2b). For the spatiotemporally distributed downscaling, we used China meteorology spatially continua gridsgrid data as observations, instead of China meteorology stations. Thestation data. We interpolated the gridded observations were interpolated to 20 km × 20 km, the same as the downscaled climate simulations. The match-up grids of simulations and observations at each time and each grid-box arewere generated.

3.1.2 Constructing relationsrelationships between the GCMs simulations and local observations

AsBecause there is an inevitable mismatch between the simulations and observations of different time and space

(Li, 2009; Wood et al., 2004) after the ~~up-sampling~~upsampling, bias correction should be performed. The bias correction was processed by ~~using~~ the ~~translation~~transform function between match-ups of the ~~up-sampled~~upsampled simulation and ~~observation~~observations, which ~~is~~represents the ~~relations of~~mapping relationship between the match-ups. The transform function could be any bias corrected model, including linear scaling, local intensity scaling, power transformation, distribution mapping models (Teutschbein et al. 2012) and other linear or nonlinear regression models.

As the influencing factors on climates show heterogeneity in space and time, we created ~~spatiotemporal~~spatiotemporally distributed ~~relations~~relationships, described by the following formula.

~~$C'_{T,S} = F_{T,S}(C_{T,S})$~~ $C'_{T,S} = F_{T,S}(C_{T,S})$ (1)

Where, ~~$C'_{T,S}$~~ $C'_{T,S}$ and ~~$C_{T,S}$~~ $C_{T,S}$ indicate the ~~up-sampled~~upsampled global-scale climate simulations and the local climate variables, respectively, in the given time of T and the space of S. ~~$F_{T,S}$~~ $F_{T,S}$ demonstrates a ~~translation~~transform function, used to correct the ~~up-sampled~~upsampled GCMs simulations. The function is a specific ~~downscaling algorithm~~bias correction model, spatiotemporally distributed in mathematic equations or parameters, which is constructed based on the data ~~in~~from the historical ~~time from~~period of 1961 to 2005.

In ~~the~~this study, we ~~created translation function based on~~use a linear-scaling algorithm (Lenderink et al., 2007~~).~~) as the bias correction model. For the linear-scaling algorithm, the simulations were corrected by the discrepancy between the simulations and observations ~~in historical time.~~. Precipitations derived from the GCMs were corrected by multiplying the precipitation bias coefficient, which is the ratio of the mean monthly observation to simulation ~~in~~from the historical ~~time; while~~period; temperatures were corrected by adding the temperature bias coefficient, which is the difference ~~value~~ between the mean monthly observation and simulation in ~~control time.~~the historical period. However, as the bias varies among the ~~Months~~months from January to December and among the locations of the 236 spatial grids, ~~the~~a global standard bias coefficient is prohibited. To better capture the bias in distributed time and space, we should create an individual bias coefficient for the given ~~Month~~month and gird box. Thus, a ~~spatiotemporal~~spatiotemporally distributed bias matrix was constructed. The respective downscaling model and bias coefficient for a given ~~Month~~month (T) and space (S) ~~was~~were established by Eq. 2 and 3.

~~$P' = P \times P\_Cof$~~ $P' = P \times P\_Cof$ (2)

~~$TM' = TM + TM\_Cof$~~ $TM' = TM + TM\_Cof$ (3)

where~~,~~ P (T) represents the precipitation (or temperature) of ~~up-sampled~~upsampled simulations. P' (TM') represents the downscaled result or ~~up-sampled~~upsampled observations; P_Cof (TM_Cof) represents the bias correction coefficient of precipitations (or temperatures). In the construction of P_Cof (TM_Cof), P (TM) and P' (TM') was set as the average monthly precipitation (or temperature) over the historical time from 1961 to 2005. All the input and output data in the equations ~~is~~are in the given ~~Month~~month (T) and space (S).

3.1.3 Correcting the GCMs simulations

The constructed relationship between the GCMs simulations and the observations ~~in~~from the historical ~~time~~period (in section 3.1.2~~), are~~) also hold for ~~data in~~ the future (Maraun et al., 2010). Thus, the ~~translation~~transform function was used to correct the future CGCMs simulations ~~in the future.~~. In ~~the~~this study, we corrected the daily and monthly precipitations (or temperatures) from MRI-CGCM3~~,~~ by adding (or multiplying) the bias coefficients in the corresponding ~~Month~~month and grid box.

3.2 Precipitation changes analysis

3.2.1 Statistic ~~indices~~indexes of precipitation changes

To obtain the general change in the temporal distribution, we calculated monthly precipitations from 1998 to

2100, averaged over the whole watershed. As ~~flood~~floods and ~~drought~~droughts occur more frequently in wet and dry months, we ~~specially~~specifically analyze the extreme wet and dry precipitation changes in the 21st century. Therein, monthly precipitations, > 75% percentile of the 12 ~~monthly precipitations~~months, were classified as the extreme wet monthly precipitations for each year of the 103 years; monthly precipitations, ⩽ 25% percentile were classified as the extreme dry monthly precipitation. The monthly precipitation of the 25%-50% and 50%-75% quantiles ~~are~~were classified as normal dry and wet monthly precipitations. The wet monthly precipitations include extreme and normal wet monthly precipitations ~~while~~; the dry monthly precipitations include extreme and normal dry monthly precipitations. To ~~further~~ understand precipitation dynamics in terms of frequency and ~~intensities~~intensity, daily precipitations were categorized into five classes based on the classification by the Chinese Meteorological Administration and the possible risk ~~to flood drought~~of floods and droughts: light rain, ~~median~~medium rain, heavy rain, rainstorm, and extreme rainstorm with daily precipitation ~~in~~of 0.1-10, 10-25, 25-50, 50-100 and >100 mm/day, respectively. The frequency of precipitation intensities indicates heterogeneity in temporal distribution. The higher frequency of moderate rain means the ~~more homogeneous~~more homogeneous, vice versa is the extreme rain. Therefore, the precipitation intensities were separated to moderate or extreme rains, including light rain, median rain or heavy rain, rainstorm, extreme rainstorm, respectively.

To ~~analysis~~further analyze the changes in precipitation frequencies and intensities, we calculate the annual days of light rain, medium rain, heavy rain, rainstorm and extreme rainstorm from 1998 to 2100 averaged over the whole watershed. Annual total precipitation, annual dry days, annual max daily precipitation and annual max ~~continual~~continuous dry days ~~are~~were displayed as well. The meteorological stations (Fig. 1a) are uniformly distributed in the whole watershed and cover all kinds of the topographies and land covers. Therefore, in the study, the all above precipitation indexes of one year for the whole watershed were calculated based on the precipitation averaged over the grids containing the 15 stations, instead of the entire grids~~, as the 15 metrological stations (Fig. 1a) are uniformly distributed in the whole watershed, covering all kinds of the topographies and land covers.~~

. Under global climate warming, precipitation becomes more ~~centred~~concentrated which leads to more heterogeneity in temporal and spatial distribution (Donat et al., 2016; Min et al., 2011). Thus, we calculated variation coefficients (VC) for each year from 1998 to 2100, to investigate the precipitation changes in temporal and spatial distribution. ~~The VC is defined by the ratio of the standard deviation and average value, described by Eq. 4.~~

The VC is defined as the ratio of the standard deviation to the average value, described by Eq. 4.

$$VC = \frac{\sqrt{\frac{\sum (x-\mu)^2}{n-1}}}{\mu} \quad VC = \frac{\sqrt{\frac{\sum (x-\mu)^2}{n-1}}}{\mu} \tag{4}$$

~~Where, x~~ where x represents monthly (or daily) precipitation ~~of~~in one year; ~~n is~~ n is the month number (or day number) of a year and ~~μ~~ μ indicates ~~averaged~~the average monthly or daily precipitation of a year. VC measures the standard dispersion of the data items, which can indicate the unevenness of ~~precipitations in~~ temporal and spatial ~~distribution.~~distributions of the precipitation. In ~~the~~this study, heterogeneity in temporal, spatial and spatiotemporal ~~distribution was~~distributions were measured by temporal, spatial and spatiotemporal VC, respectively. Temporal VC was calculated on the daily or monthly precipitations in one year~~, where~~ and the VC for one year is averaged over ~~that~~those of the 15 stations. For monthly precipitation, we only select extreme wet and dry precipitations, as the extreme wet and dry are more likely to cause floods or droughts and thus should be ~~pay~~paid more ~~attractions to.~~attention. Spatial VC ~~were~~was calculated on the annual total precipitations of the 15 stations in one year. Spatiotemporal VC was calculated on the monthly precipitations of the extreme wet months of the wet stations and the extreme dry months of the dry stations in one year, as the extreme precipitation ~~value was~~values were more likely to cause floods or droughts.

3.2.2 Relationship analysis between precipitation changes and temperature increasing

We investigated the precipitation changes as a result of global temperature increase. To this end, we made liner regression between the precipitation index and temperature changes from 2005 to 2100. We note that a mean filter with a ~~widow~~window size of 21 years can reduce potential random fluctuation from precipitation by the most; thus was used to smooth annual precipitation indexes and temperature simulations from 2005 to 2100. The long-time smoothed annual precipitation or temperature minus the average annual value from 1998 to 2017, are set as precipitation index or temperature changes. A linear regression model was used to investigate whether precipitation changes are related to climate warming. The two 11 years, 2005 to 2015 and 2090 to 2100 at the start and end, did not have filter diameter of 21 years; thus climate data used to be regressed is from 2016 to 2089.

4 Result and Discussion~~–~~

4.1 ~~Validations of precipitation~~Model assessment

Validation about the China meteorological grid observations should be performed, as well as the STDDM. As the STDDM introduce the China meteorological grid observations and ~~temperature projections~~the grid data is not the direct in ~~Poyang Lake Watershed~~

~~Before being used in future climate projection, the model was examined. Data from 1961 to 1985 were used to construct the model, and the remaining historical data from 1986 to 2005 were used to validate.~~ -suit data, validation about the gridded data is necessary. The determination coefficient (R2), root mean square error (RMSE) and PBias (percent bias) were used to examine the model performance.~~–~~

4.1.1 Evaluation for the gridded meteorological

The China meteorological grid observations are referenced data to corrected GCMs simulations and reliability of the observations is vital to the performance of the STDDM. So we make a validation using meteorological station observations, in Fig. 3.

As shown in Fig. 3, we select four meteorological stations. The selected stations are uniformly distributed. The validation produced an acceptable precision with $R^2 > 0.91$, absolute PBias < 2% for precipitations and $R^2 = 0.99$, absolute PBias < 6% for temperature. All the dots of gridded and stationed value were distributed along the 1:1 line, thus confirming the satisfactory performance.

4.1.2 Validations of precipitation and temperature projections in Poyang Lake Watershed

Before being used in future climate projection, the model should be examined. Data from 1961 to 1985 were used to construct the model, and the remaining historical data from 1986 to 2005 were used to validate.

To test whether the downscaling method (STDDM) is effective in climate projections, we compare the results before and after the bias correction in Fig. ~~3.~~4. The results before and after the bias correction marked as the outcomes by the STDDM and No-STDDM, respectively. The projections ~~with bias corrections~~by the STDDM show better performance with high correlations and narrow bias, compared to the result ~~without bias corrections.~~by No-STDDM. Considering the complexity of climate physical mechanism~~, which is difficult~~ and difficulty to accurately ~~simulated~~simulate by the present methods, the uncertainty could be acceptable.

Using the STDDM and MRI-CGCMs, we obtained the temporal and spatial variation of future precipitations in the Poyang Lake Watershed, and investigated the heterogeneity changes of precipitation in the temporal and spatial distribution.

4.2 Temporal variation of future precipitation

~~**4.1.1 Monthly scale**~~

To ~~facilitate discovering~~ discover the ~~general intra- and inter-annual variability over~~temporal variation under the future climate warming, we ~~analysed~~analyzed the monthly and daily precipitation changes during the period from 1998 to 2100. For monthly precipitation, we analyzed intra-annual and inter-annual dynamics of precipitation; based on the dynamics, we investigated the heterogeneity changes of monthly precipitation. For daily precipitation, we analyzed the changes of precipitation intensities and frequencies; based on the changes, heterogeneity changes of daily precipitation was also investigate.

4.2.1 Monthly precipitation changes

We analyzed the monthly precipitation changes during the period from 1998 to 2100 in Fig. ~~4~~5. Precipitation ~~gathered in spring (March to May) and summer (July to August), occupying 73% of the annual amount, which highlights the~~ show significant intra-annual dynamics ~~of rains. Rich~~. Months with abundant rain (wet months~~;~~), indicated by a reddish color, are mainly in April to July (the wet season~~);~~), while the rain-poor ~~rain~~ months (dry months), indicated by a bluish color, are mainly in September to ~~next~~the subsequent February (the dry season). Precipitation concentrates in spring (March to May) and summer (July to August), occupying 73% of the annual amount. The intra-annual dynamics of ~~precipitations~~ precipitation is similar to that ~~of the~~shown by Feng~~'s~~ (2012). ~~In the~~Precipitation also showed inter-annual ~~precipitation pattern, the rich rain~~dynamics. The wet months become ~~richer~~wetter, and the ~~rich rain~~wet season comes earlier from April to March, even in February. ~~Precipitations~~ In addition, each monthly precipitations of seven months (April to November) took increasing trends, of which ~~71%~~most months (5 ~~out of the 7~~ months; April, May, June, August) are in the wet season; while precipitations of the other five months experienced decreasing trends ~~and~~, all ~~the months~~of which were in the dry season. It seems that wet months become wetter and dry months become drier, in general.

~~The monsoon is the dominant factor to inter or intra annual variability of precipitation. The reaching time of the monsoon reaching Poyang Lake Watershed, varies in different years, with 1~2 months' advance or delay. Therefore, the rich or poor rain months for different years are not the same.~~ To better demonstrate the ~~opposite variations (the decreases in the dry period and increases in wet);~~inter-annual dynamics of precipitation, monthly precipitations in each year were sorted in ~~the~~a descending order in Fig. ~~4~~5(b). ~~Wet monthly precipitations~~As the time of the monsoon reaching the Poyang Lake Watershed, varied in different years, with 1~2 months' advance or delay; the wet or dry months for different years are not the same. By sorting monthly precipitation, wet months and dry month could be distinguished intuitively in Fig. 5(b). Obviously, monthly precipitation of wet months experienced an increasing trend respectively, even ~~with~~ some ~~significant sign; whereas~~with slight significance; in contrast, each dry monthly precipitation exhibited decreasing trends, separately, despite the insignificant signs. We accumulated the extreme wet or dry monthly precipitations for each year in Fig. ~~5~~6. The precipitation of extreme wet months showed a significantly increasing trend ($p<0.05$) (Fig. ~~5a), and~~6a), while the precipitation of the extreme dry months demonstrated a significantly decreasing trend ($p<0.05$). Extreme wet months increased from 277.82 mm•month^{-1}/a over historical time from 1998-2017, to 344.10 mm•month^{-1}/a over future time from 2081 to 2100, by 23.86~~%~~ with a change rate of 7.3 mm•month^{-1}/10a~~; while the precipitation of extreme~~. Extreme dry months ~~demonstrated a significantly decreasing trend ($p<0.05$) (Fig. 5b) and~~ decreased from 35.44 mm•month^{-1}/a over historical time from 1998-2017, to 30.46 mm•month^{-1}/a over future time from 2081 to 2100, by -14.05~~%~~ with a change rate of 0.92 mm•month^{-1}/10a. Therein, the extreme wet months are mainly concentrated in March-July (Fig. ~~5c~~6c), part of the wet season~~;~~, while the extreme dry months are mainly concentrated in September-February (Fig. ~~5d~~6d), consistent to the dry season.

Overall, ~~with~~under climate warming over the ~~21~~21st century, the wet monthly precipitations become wetter while the dry month precipitations become ~~dryer~~drier, which ~~highlights~~suggested the uneven temporal distribution of precipitation (Fig. ~~6~~7). As shown in Fig. ~~6~~7, the temporal variation coefficient of the extreme month (including extreme wet and months) precipitations within each year from 1988 to 2100, experiences significantly increasing trends ($p<0.01$), and increased from 0.76 /a over historical time from 1998-2017, to 0.84 /a over future time from

2081 to 2100, by 10.53% with change rate of 0.01 /10a. The significantly increasing trends indicated the more uneven trend of precipitation in the temporal distribution, which might lead to ~~increasing~~increased risks of floods and droughts.

4.~~1~~2.2 Daily ~~scale~~precipitation changes

To understand the changes ~~of~~in precipitation intensities and frequencies under ~~the~~ future climate warming, daily precipitation variations were also ~~analysed~~analyzed and are shown in Fig. ~~7. Averaged over 103 years, annual precipitation~~ 8. Moderate vs extreme rain frequencies ~~are dominated by~~(Fig. 8a and b), the ~~moderate rain, a~~annual total ~~of 163.70~~rain vs the annual total rainy days~~, 44.8 % (163.70/365) while~~ (Fig. 8c), and the ~~extreme rain occurs less often, a total of 20.70~~annual max precipitation vs the annual max continuous rainy days~~, 6.70 % (20.7/365).~~ (Fig. 8d) were analyzed.

Under~~The remaining is rain-free days, a total of 180.75 days, 49.5% (180.75/365). Over the~~ climate warming, the annual frequency of moderate rains experienced decreasing trends; in contrast, the annual frequency of extreme rains experienced significantly increasing trends (Fig. ~~7a~~8a). Statistically, ~~the~~ averaged over 103 years, annual precipitation frequencies are dominated by the moderate rain frequency a total of 163.70 days, or 44.8% (163.70/365), while the extreme rain occurs less often, a total of 20.70 days, or 6.70% (20.7/365). The remaining is rain-free days, a total of 180.75 days, 49.5% (180.75/365). ~~was~~ The annual moderate rain frequency decreased, from 170.56 days/a over the historical ~~time from1998~~period from 1998 to 2017, to 159.55 days/a over the future ~~time~~period from 2081 to 2100, by -6.46% with a change rate of -14.4 days/10a; ~~while~~on the contrary, the annual extreme rain frequency ~~was~~ increased from 19.18 days/a over historical time from1998 to 2017, to 23.42 days/a over future time from 2081 to 2100, by 22.10~~-~~% with a change rate of 0.49 days/10a (Fig. ~~7b~~8b).

~~The~~ Furthermore, the annual total rainy days, the sum of the moderate and extreme ~~rains~~rain frequencies, demonstrated a significantly decreasing ~~trends~~trend in the 21st century~~;~~, whereas the annual total precipitation exhibited a significantly increasing trend (Fig, 7c). Rainy days ~~were~~ decreased from 187.57 days/a over the historical ~~time from1998~~period from 1998 to 2017, to 180.37 days/a over the future ~~time~~period from 2081 to 2100, by -3.84% with a change rate of -1.00 days/10a; while the annual total rain amount ~~was~~ increased, from 1650 mm/a over the historical ~~time~~period, from 1998 to 2017, to 1906 mm/a over the future ~~time~~period, from 2081 to 2100, by 15.55~~-~~% with a change rate of 23.~~00mm~~00 mm/10a. The ~~increasing~~increase in the annual total rain and ~~decreasing~~decrease in the annual rainy days suggested more concentrated precipitation and dry days~~. The~~ in the future. This tendency might lead to ~~increasing~~ the increased risk of ~~flood drought~~floods and droughts, which was also ~~documented~~indicated by the ~~increasing~~increased annual max daily precipitation and max continuous dry days (Fig. ~~7d).~~8d). Annual max daily precipitation ~~was~~ increased from 148.76 mm•day^{-1}/a averaged over the historical ~~time from1998~~period from 1998 to 2017, to 212.01 mm•day^{-1}/a averaged over the future ~~time~~period from 2081 to 2100, by 42.51% with a change rate of 7.2 mm•day^{-1}/10a; while the max continuous dry days ~~was~~ increased from 25.35 days/a over the historical ~~time~~period from 1998 to 2017, to 28.15 days/a over the future ~~time~~period from 2081 to 2100, by 11.05% with a change rate of 0.5 days/10a.

Overall, the significantly inverse change ~~tends~~trends in the moderate vs extreme rain frequencies, the annual total rain vs the annual total rainy days, and the annual max precipitation vs the annual max continuous rainy days, indicated an increasing temporal heterogeneity in precipitation distribution over the 21st century. Obviously, the increasing heterogeneity was ~~also~~ exhibited by the increasing temporal VC of daily precipitations (Fig. ~~8~~9). The temporal VC of daily ~~precipitation was~~precipitations increased from 1.50 /a over the historical ~~time from1998~~period from 1998 to 2017, to 1.62 /a over the future ~~time~~period from 2081 to 2100, by 7.48% with a change rate of 0.016 /10a.

4.3 Spatial variation of future precipitation

Climate warming could cause the rain belt shift (Putnam et al., 2017), which might lead to precipitation changes in the spatial pattern. ~~The~~ To investigate the spatial variation ~~was~~, we analyzed ~~in~~ the similarities and differences of precipitation changes in space (Fig. ~~9 and 10. As floods~~ 1); based on the differences, we use the indexes of the spatial and ~~droughts occur more frequently in extreme months, the precipitation in the analysis considered only~~

the extreme wet (April-July) and dry (September-February) monthsspatiotemporal VC to investigate the spatial heterogeneity changes (Fig. 11). Fig. 5c and d). Besides, 10 shows the precipitation is dominated by southeast summer monsoon, which bring water vapour from the sea.changes in The summer monsoon is frequent from the end of spring and stat of autumn, covering the wet months April to July. However, though as dry months, the autumn period from September to November is affected by southeast summer monsoon (Tan et al., 1994) slightly because autumns are the transpiration periods of summer to winter. Therefore, winter (December-February) was represented as the dry season with poor rain; while April-July was represented as the wet season with rich rain. To visualize the spatial pattern of the precipitation changes in the wet and dry season under future climate warming, we calculated the mean wet or dry precipitation averaged over the historical during the period from 1998 to 2017 (Fig. 9a or d), the near future period from 2041 to 2060 (Fig. 9b or e), and the further future period from 2081 to 2100 (Fig. 9c or f), respectively. The change rate of wet or dry season precipitation from 19982100; Fig. 11 shows the spatial and spatiotemporal VC for each year over 1988 to 2100 (Fig. 9g or h) were also exhibited the climate warming impacts on the spatial pattern of precipitation changes.

PrecipitationsAs shown in Fig. 9a-c and e-g, precipitations showed a regular spatial pattern both in the wet and dry season., in Fig. 10a-c and e-g. More specifically, precipitations were precipitation was distributed more in the east and west, whichhowever less in the north central plain and the south bottom depression. Rich rain in the east and west are dominated by the southeast and southwest summer monsoon. Whereas, precipitations were distributed less in the north central plain for reasons of being as monsoons. Less precipitation was due to the leeward sloop of the easteastern (Xuefeng Mountain) and west mountainwestern mountains (Wuyi Mountain), and). Less precipitation in the south bottom depression due towas because that the water vapor was blocked from this region by the NanLing Mountain in the south (Fig. 1a). The precipitation distribution in spatial pattern from 1998 to 2100 (Fig. 910 a-c and d-f) were consistent towith the observations from 1951 to 2005 (Fig. 1b.), thus confirming the satisfactory performance of the STDDM. Moreover, wet and dry season precipitation showed inverse changes. The wet season precipitations exhibited ascending (Fig. 10a-c and g) change while the dry season precipitation exhibited descending (Fig. 10d-f and h) change from 1998 to 2100. The inverse changes were consistent with the interannual variability of increased precipitation in wet months and decreased precipitation in dry months (Section 4.2). The increase of precipitation in the wet seasons and decrease in precipitation in the dry seasons were also detected in the change rate of the cells over the entire watershed (Fig. 10g or h).

Yet, wet and dry season precipitations showed inverse changes. The inverse is consistent with the inter-annual variability of increasing However, precipitation trend in wet months and decreasing trend in dry months (Section 4.2). The wet or dry season precipitations exhibited ascending (Fig. 9a-c and g) or descending (Fig. 9d-f and h) change from 1998 to 2100, respectively. Specifically, the wet season precipitation was increased from 172.5-266.3 mm•month^{-1}/a averaged over the historical time (1998-2005), 189.9-265.3mm•month^{-1}/a averaged over the near future (2041-2060), to 219.9-345.8mm•month^{-1}/a averaged over the further future (2081-2100), with an increasing change of 3.5-11.7mm•month-1/10a, range in the cells of the whole watershed (Fig. 9 a-c, g). In contrast, the dry season precipitation was decreased from 68.4-99.9mm•month^{-1}/a averaged over the historical time (1998-2005), 66.5-99.0 mm•month^{-1}/a averaged over the near future (2041-2060), to 56.7-84.9 mm•month^{-1}/a averaged over the further future (2081-2100), with an decreasing change of -2.7--1.1mm•month^{-1}/10a, range in the cells of the entire watershed (Fig. 9 d-f, h). The tendency of being wetter in wet seasons and drier in dry seasons might lead to increasing risks of floods and droughts.

The increase of precipitation in wet seasons or decrease in dry seasons were also detected in the cells over the entire watershed (Fig. 9g or h). However, the spatial patterns of changes are complex with regionally different signs (Fig. 9g and h). The wet season precipitation increase was different in spatial distribution, with change rate raising from ⩽3.6 mm/10a in the southwest, to ⩾11.7 mm/10a in northeast; while the decrease of the dry season precipitation in falls from ⩾ -2.0 mm/10a in the surroundings, to ⩽ -2.7 mm/10a in the centre.showed a different spatial pattern. Precipitation change rate was heterogeneous in spatial distribution for dry or wet season respectively (Fig. 10g and h). In the wet season, the precipitation increased more in the north part of the watershed, except for the centrecentral plain (Fig. 9g); while10g); in the dry season, the precipitation decreased more in the centercentral area (Fig. 9h). The uneven change rates indicated the increasing heterogeneity of

precipitations in the spatial distribution (10h). Statistically, in the wet season, precipitation increased with the change rate raising from ⩽ 3.6 mm/10a in the southwest, to ⩾ 11.7 mm/10a in the northeast; in the dry season, precipitation decreased with the change rate falling from ⩾ -2.0 mm/10a in the surrounding region, to ⩽ -2.7 mm/10a in the central region. FurthermoreFig. 10a). Specifically, the heterogeneity was raised with the spatial VC increasing from 0.097/a over historical time from1998 to 2017, to 0.110/a over future time from 2081 to 2100, by 12.64% with a change rate of 0.002/10a.

However, precipitation changes show a different spatial pattern betweencharacteristics in wet and dry seasons. From 1998 to 2100, in the wet season (Fig 9a. 10a-c), the wet area (the reddish area, mainly in the north except for the center plain) becomebecomes wetter; while in the dry season (Fig. 910 d-f), the dry area (the bluish area, mainly in the north center plain and in the south depression) become drier. The tendency of being wetter in The uneven change rates may lead to increase of the spatial heterogeneity of precipitation under global warming, and the tendency of the wet area to become wetter and drier in the dry area might enhance the risk of floods and droughts. The drier condition in the dry season and area and wetter condition in the wet season and areato become drier also indicated the increasing heterogeneity of precipitations in the spatiotemporal distribution (heterogeneity of precipitations. Indeed, the spatial heterogeneity did increase, with the spatial VC raising from 0.097 /a over the historical period (1998-2017), to 0.110 /a over the future period (2081-2100), by 12.64% with a change rate of 0.002 /10a (Fig. 11a). The spatiotemporal Fig. 10b). Specifically, the heterogeneity was raiseddid increase with the spatiotemporal VC increasingraising from 0.89 /a over the historical time from1998 to period (1998-2017,), to 0.94 /a over the future time from period (2081 to -2100,), by 4.96% with a change rate of 0.008/10a. /10a. Overall, the uneven change rates for the whole basin and inverse changes for the dry and wet area indicated an increasing spatial heterogeneity in precipitation distribution over the 21st century.

4.4 The impact assessment of temperature increasingincrement on precipitation changes

Previous studies have detected precipitation changes, and attributehave attributed these changes to climate warming (Westra et al., 2013; Zhang et al., 2013). In thethis study, the spatiotemporal changes of precipitation in the Poyang Lake Watershed in the 21st century were supposedhypothesized to be related to the increasing temperature. increments. So we analyze the correlations qualitatively and quantitatively.

The following are trying to demonstrate the driving force related to climate warming on precipitation changes in the temporal pattern. In the wet season from April to July, the summer monsoon might becomesbecome weaker in the southeast ofSoutheast Asia, with as the climate warmingtemperature increasing (Wang, 2001; Wang, 2002; Guo et al., 2003). Consequently, the summer monsoon delaysis delayed for a longer time in the middle and lower Yangtze River basin for a longer time, instead of moving further north. The delays leaddelay leads to much more rain during the wet season. LocatedAs being located in the middle of the Yangtze River basin, the Poyang Lake Watershed becomes wetter in the wet season (Fig. 45-5, Fig. 9a10a-c). In fact, the increase ofin precipitation in the Poyang Lake Watershed was detected in previous studies (Yu and Zhou, 2007; Ding et al., 2008). In the poor-raindry period from September to nextthe subsequent February (especially in the winter timeseason, from December to February) with low-frequency), during which summer monsoon is inactive, there is less water vapor in atmospheres, which is not easy to the atmosphere to condense into rain. Additionally, stronger winds in the winter (Wu et al., 2013) blow the evaporation away. The stronger wind in winter enhances, thus enhancing the difficulty to gather enough of generating rain from water vapor to rain, compared to the other seasons. When temperature increases over the 21st century, the atmospheres, the ability of holdingthe atmosphere to hold water vapors is strengthened, which makemakes it more difficult to precipitate. Therefore, precipitations decreaseprecipitation decreases in the dry season, similar toconsistent with Li et al.'s (2016) researchresult. As climate warmingtemperature increment increases the ability of the atmosphere to contain water vapor, it is harder to condense into rain onlyis more difficult, and if it has enough more water vaporrains it will rain largely (Min et al., 2011; Zhang et al., 2013). Thus, the frequency of heavy rain and rain-free rain events increases, which indicates moreindicating increased frequency and strengthened intensity of the extreme rains and less of moderate rains. Overall, climate warming might make precipitation. Overall, the climate warming might make precipitation more temporally uneven in temporal distribution.

Climate warming could also explain the spatial distribution of precipitation ~~change~~changes in the dry and wet seasons. In the wet season, the summer monsoon delays in the middle and lower Yangtze River Basin. The delaying area covers only the north part of the Poyang Lake Watershed. ~~Because of getting rich~~As it receives abundant water vapor from the delayed summer monsoon, ~~precipitation in~~ the north part of Poyang Lake Watershed ~~are increased more with~~ experiences a greater increase in precipitation with a larger change rate (Fig. ~~9g~~10g). The ~~east of~~eastern Poyang Lake Watershed is the nearest to the ~~sea, west of~~western Pacific Ocean; thus the ~~east can get~~eastern region receives more continuous water vapor ~~continually. That's why~~. So the precipitation change rate decreases from the southeast to the northwest~~.~~ in the wet season. However, in the dry season especially in winter, during which there is ~~with~~a low-frequency or ~~even no~~absent summer monsoon, the water vapor mainly comes from evapotranspiration. In the watershed, ~~there is more evapotranspiration in~~ the periphery~~, which~~ is covered by the lake of Poyang in the northern plain and high-density vegetation in the northwest, southeast~~,~~ and southwest mountains~~, and lake of Poyang in the north plain; while~~; so there is ~~less~~more evapotranspiration in the periphery. The center~~,~~ is mainly covered by farmland and grassland; so there is less evapotranspiration in the center (Wu et al., 2013). Thus, the moisture decreases from the ~~surroundings~~surrounding to the center. Therefore, ~~it is more difficult to rain in lower moisture area, the center part of Poyang Lake Watershed as~~ as temperature increases~~; thus~~, it is more difficult for rain to occur in the area of lower moisture, the center of the Poyang Lake Watershed. Therefore the precipitation ~~decreasing~~decreased with a change rate falling from the ~~surroundings~~surrounding to the center in the dry season (Fig. ~~9h~~10h).

To quantitatively analyze the relationship between precipitation changes and temperature ~~increasing~~increment, we ~~made~~created a scatter plot between precipitation indexes changes and temperature ~~increases~~increment, as shown in Fig. ~~11. Trend~~12. A trend analysis was conducted ~~by~~using linear regression ~~over~~of each annual precipitation ~~indexes against~~index over the 103 years from 1998 to 2100. The associated slopes ~~represented~~represent the change rate ~~for~~of each ~~long-term~~ precipitation ~~indexes.~~index relative to temperature increment. The significance of the trend ~~significant sign was~~is indicated by p value. As shown in Fig. ~~11~~12, there is ~~statically~~a significant ~~correlations~~correlation between the precipitation ~~changes~~change and the temperature ~~increasing~~increment, with ~~significant sign of~~ $p \leqslant 0.001$ and $R \geqslant 0.78$ for 6 precipitation indexes~~,~~: the annual precipitation in the wet season (Fig. ~~11a),~~12a), the annual max daily precipitation (Fig. ~~11d),~~12d), the temporal VC of the monthly precipitation (Fig. ~~11c),~~12c), the temporal VC of the daily precipitation (Fig. ~~11f),~~12f), the spatial VC (Fig. ~~11g~~12g) and the spatiotemporal VC (Fig. ~~11h~~12h). However, ~~the change~~changes of the other two precipitation indexes, the annual precipitation in the dry season (Fig. ~~11b~~12b) and the annual max ~~continual~~continuous dry days (Fig. ~~11c~~12e), appeared to be correlated with slight signs of $p \leqslant 0.05$ and $R \leqslant 0.58$. The overestimation of ~~light~~moderate- or free-rain frequency from the GCM simulations (Teutschbein et al. 2012) might ~~explains~~explain the ~~slight correlations for~~ slightly low correlation between the annual precipitation values in the dry season~~;~~ and temperature increment, while the overestimation of the precipitation frequencies (Prudhomme et al. 2003) could ~~be~~explain the ~~reason of the slight~~slightly low correlation ~~for~~between the annual max ~~continual~~continuous dry days~~.~~ and temperature increment. For all the correlations (Fig. ~~11a~~12a-h), the precipitation changed with fluctuation, which might be caused by random variations ~~of~~from GCMs.

~~Despite~~Overall, despite the ~~slight signs~~low correlations and stochastic fluctuation, the correlations ~~exhibited~~could indicate that the climate warming can partly ~~explained~~explain the precipitation changes~~, with variations of~~. Statistically, precipitation changes relative to temperature increment are 16.657 mm•month^{-1}/K, -4.31 mm•month^{-1} /K, 17.45 mm•day^{-1} /K, 0.71 days/K, 0.028/K, 0.033/K, 0.0074/K and 0.02/K for the annual precipitation in the wet season, the annual precipitation in the dry season, the annual max daily precipitation, the annual max ~~continual~~continuous dry days, the temporal VC of the monthly precipitation, ~~and~~the temporal VC of the daily precipitation, and the spatial VC and the spatiotemporal VC, respectively.

In summary, the explanation of precipitation changes in temporal and spatial distribution qualitatively and quantitatively, suggests the downscaling method is reasonable and the STDDM could be applied in the basin-scale region based on a GCM successfully.

5 Conclusion

A ~~spatiotemporal~~spatiotemporally distributed downscaling method (STDDM) was proposed in this study. The downscaling method considered the heterogeneity in spatial and temporal distributions, and produced local climate variables as ~~spatial~~spatially continuous data instead of independent and discrete points. ~~The~~The STDDM showed a better performance than the No-STDDM. Using the STDDM, we constructed the spatially continuous future precipitation distribution and dynamics in the wet and dry season ~~are constructed and several~~from 1998 to 2100, based on MRI-CGCM3. Several findings ~~are~~were obtained~~.~~:

~~Firstly~~First, the spatial and temporal heterogeneity of precipitation ~~in the spatial and temporal pattern is enhanced~~ increased under future climate warming. In the temporal pattern, the wet season ~~precipitation increased with change rate of 7.33 mm/10a and 11.66 mm/K;~~become wetter, while the dry season ~~precipitation decreased with change rate of −0.92 mm/10a and −4.31 mm/K.~~become drier. The frequency of extreme precipitation ~~frequency and intensity were strengthened with change rate~~increased, while that of ~~0.49~~the moderate precipitation decreased. Total precipitation increased, while rain days~~/10a and 7.2mm•day^{-1}/a.~~ decreased. The ~~inverse changes in the~~ max dry ~~and wet season,~~day number and the ~~increasing extremes frequencies~~ max daily precipitation both increased. These precipitation changes demonstrated an ~~ascending~~increasing heterogeneity of precipitation in temporal distribution, ~~with~~and the change rate of temporal heterogeneity is 0.01 /10a (~~0.028/K) or~~ 0.016 /10a ~~(0.033/K~~) for the temporal VC of the monthly ~~or~~ (daily) precipitation. In the spatial pattern, the ~~uneven change rates of the entire cells covering the watershed demonstrated an increasing heterogeneity in spatial distribution, with the change rate of 0.002/10a (0.0074/K) for the spatial VC. In the spatiotemporal pattern~~change rate of precipitation was uneven over the whole watershed. Additionally, the wet areas become wetter in the wet season and the dry areas become drier in the dry season~~, which manifested~~. The uneven change rates for the whole basin and inverse change for dry and wet area demonstrated an increasing heterogeneity in the ~~spatiotemporal~~spatial distribution, and the change rate of spatial heterogeneity was 0.002/10a ~~(0.02/K) respectively.~~

~~Secondly, analysis with temperature increases showed that~~ Second, precipitation changes ~~in the spatial and temporal pattern appear to be significantly related to the climate warming. Precipitation changes~~ can be significantly explained by ~~temperature increasing~~climate warming, with $p < 0.05$ and $R \geqslant 0.56$. The ~~variability of annual precipitation in the wet season, annual precipitation in the dry season, annual max daily precipitation, annual max continual dry days, temporal VC of monthly~~ explanation of precipitation~~, and temporal VC of daily precipitation, spatial VC and spatiotemporal VC, are 16.657 mm/K, −4.31 mm/K, 0.028/K, 17.45 mm/K, 0.71 days/K, 0.033/K, 0.0074/K and 0.02/K, respectively~~ changes in temporal and spatial distribution qualitatively and quantitatively, suggests the downscaling method is reasonable and the STDDM could be applied in the basin-scale region based on a GCM successfully.

~~This study demonstrates the precipitation changes under climate warming in the 21st century. The wetter condition in the wet season and drier condition in the dry season are expected to cause an increased risk of floods and droughts in the future.~~ The results can be applied to a hydrological and hydrodynamic model, to study the future changes ~~of~~in water ~~resource~~volumes, lake ~~level~~levels and ~~area~~areas response to climate warming. The relationship between precipitation variations and temperature ~~increasing~~increment could be helpful to the driving ~~force~~forces analysis ~~on rainfall~~of precipitation changes. ~~Furthermore, for~~The dry to be drier and wet to be wetter condition may lead to increased risk of floods and droughts. In particular, in the region where floods and droughts ~~did~~do not usually occur ~~frequently~~, additional adaptation measures could be taken to prevent loss from ~~more~~the future frequent ~~and serious~~ hydrological disasters.

Data availability

All data can be accessed as described in Sect. 2.2. The data sets and model codes are provided in the supplements.

Acknowledgements

This work was funded by the National Natural Science Funding of China (NSFC) (41331174, 41461080), the National Key Research and Development Program (2017YFB0504103), the Open Foundation of Jiangxi Engineering Research Center of Water Engineering Safety and Resources Efficient Utilization (OF201601), the ESA-MOST Cooperation DRAGON 4 Project (EOWAQYWET), the Fundamental Research Funds for the Central Universities (2042018kf0220) and the LIESMARS Special Research Funding.

Reference

Alexander, L. V., Zhang, X., Peterson, T. ., Caesar, J., Gleason, B., Klein Tank, A. M. G., Haylock, M. R., Collins, W. D. and Trewin, B.: Global observed changes in daily climate extremes of temperature and precipitation, J. Geophys. Res., 111, D05109, doi:10.1029/2005JD006290, 2006.

Baigorria, G. A. and Jones, J. W.: GiST: A Stochastic Model for Generating Spatially and Temporally Correlated Daily Rainfall Data, J. Clim., 23(22), 5990–6008, doi: 10.1175/2010jcli3537.1, 2010.

Beven, K. J.: A Discussion of distributed hydrological modelling, Distrib. Hydrol. Model., 255–278, doi:10.1007/978-94-009-0257-2_13, 1996.

Chen, H. and Sun, J.: How the “best” models project the future precipitation change in China, Adv. Atmos. Sci., 26(4), 773–782, doi:10.1007/s00376-009-8211-7, 2009.

Chu, J. T., Xia, J., Xu, C. Y. and Singh, V. P.: Statistical downscaling of daily mean temperature, pan evaporation and precipitation for climate change scenarios in Haihe River, China, Theor. Appl. Climatol., 99(1–2), 149–161, doi:10.1007/s00704-009-0129-6, 2010.

Dai, A.: Increasing drought under global warming in observations and models, Nat. Clim. Chang., 3(1), 52–58, doi:10.1038/nclimate1633, 2013.

DHI (Danish Hydraulic Institute): MIKE SHE, User Manual, Volume 1: User Guide. Hørsholm: Danish Hydraulic Institute, 2014.

Dyderski, M. K., Paź , S., Frelich, L. E. and Jagodziński, A. M.: How much does climate change threaten European forest tree species distributions?, Glob. Chang. Biol., doi:10.1111/gcb.13925, 2017.

Engman, E. T.: Remote sensing in hydrology, Geophys. Monogr. Ser., 108, 165–177, doi:10.1029/GM108p0165, 1998.

Enke, W., Schneider, F. and Deutschländer, T.: A novel scheme to derive optimized circulation pattern classifications for downscaling and forecast purposes, Theor. Appl. Climatol., 82(1–2), 51–63, doi:10.1007/s00704-004-0116-x, 2005.

Feng, L., Hu, C., Chen, X., Cai, X., Tian, L. and Gan, W.: Assessment of inundation changes of Poyang Lake using MODIS observations between 2000 and 2010, Remote Sens. Environ., 121, 80–92, doi:10.1016/j.rse.2012.01.014, 2012a.

Feng, L., Hu, C., Chen, X., Tian, L. and Chen, L.: Human induced turbidity changes in Poyang Lake between 2000 and 2010: Observations from MODIS, J. Geophys. Res. Ocean., 117(7), doi:10.1029/2011JC007864, 2012b.

Giorgi, F.: Simulation of Regional Climate Using a Limited Area Model Nested in a General Circulation Model, J. Clim., 3(9), 941–963, doi:10.1175/1520-0442(1990)003<0941:SORCUA>2.0.CO;2, 1990.

Giorgi, F.: Simulation of Regional Climate Using a Limited Area Model Nested in a General Circulation Model, J. Clim., 3(9), 941–963, doi:10.1175/1520-0442(1990)003<0941:SORCUA>2.0.CO;2, 1990.

Grotch, S. L. and MacCracken, M. C.: The Use of General Circulation Models to Predict Regional Climatic Change, J. Clim., 4(3), 286–303, doi:10.1175/1520-0442(1991)004<0286:TUOGCM>2.0.CO;2, 1991.

Guo, J.L., Guo, S., Guo, J., Chen, H.: Prediction of Precipitation Change in Poyang Lake Basin. Journal of Yangtze River Scientific Research Institute, 8, 007, 2010.

Han, X., Chen, X. and Feng, L.: Four decades of winter wetland changes in Poyang Lake based on Landsat observations between 1973 and 2013, Remote Sens. Environ., 156, 426–437, doi:10.1016/j.rse.2014.10.003, 2014.

Hong X, Guo S, Guo J, et al. Projected changes of extreme precipitation characteristics in the Poyang Lake Basin based on statistical downscaling model. Journal of Water Resources Research, 3(6), 511-521,

doi:10.12677/JWRR.2014.36063, 2014.
Lenderink, G., Buishand, A. and Van Deursen, W.: Estimates of future discharges of the river Rhine using two scenario methodologies: Direct versus delta approach, Hydrol. Earth Syst. Sci., 11(3), 1145–1159, doi:10.5194/hess-11-1145-2007, 2007.
Li, H., Sheffield, J. and Wood, E.: Bias correction of monthly precipitation and temperature fields from Intergovernmental Panel on Climate Change AR4 models using equidistant quantile, J. Geophys. Res., 115(10), D10101, doi:10.1029/2009JD012882, 2010.
Li, Y. L., Tao, H., Yao, J. and Zhang, Q.: Application of a distributed catchment model to investigate hydrological impacts of climate change within Poyang Lake catchment (China), Hydrol. Res., 47(S1), 120–135, doi:10.2166/nh.2016.234, 2016.
Liu, C. M., Liu, W. Bin, Fu, G. Bin and Ouyang, R. L.: A discussion of some aspects of statistical downscaling in climate impacts assessment, Shuikexue Jinzhan/Advances Water Sci., 23(3), 427–437, doi:CNKI: 32.1309.P.20120501.1616.002, 2012.
Lohmann, D., Rashke, E., Nijssen, B. and Lettenmaier, D. P.: Regional scale hydrology: I. Formulation of the VIC-2L model coupled to a routing model, Hydrol. Sci. J., 43(1), 131–141, doi:10.1080/02626669809492107, 1998.
Min, Q., Min, D.: Drought Change Characteristics and Drought Protection Countermeasures for Poyanghu Lake Basin, Journal of China Hydrology, 1, 84-88, 2010.
Min, S. K., Zhang, X., Zwiers, F. W. and Hegerl, G. C.: Human contribution to more-intense precipitation extremes, Nature, 470(7334), 378–381, doi:10.1038/nature09763, 2011.
Mullan, D., Chen, J. and Zhang, X. J.: Validation of non-stationary precipitation series for site-specific impact assessment: comparison of two statistical downscaling techniques, Clim. Dyn., 46(3–4), 967–986, doi:10.1007/s00382-015-2626-x, 2016.
Pall, P., Aina, T., Stone, D. A., Stott, P. A., Nozawa, T., Hilberts, A. G. J., Lohmann, D. and Allen, M. R.: Anthropogenic greenhouse gas contribution to flood risk in England and Wales in autumn 2000, Nature, 470(7334), 382–385, doi:10.1038/nature09762, 2011.
Prudhomme, C., Reynard, N. and Crooks, S.: Downscaling of global climate models for flood frequency analysis: Where are we now, Hydrol. Process., 16, 1137–1150, 2002.
Putnam, A. E. and Broecker, W. S.: Human-induced changes in the distribution of rainfall, Sci. Adv., 3(5), doi:10.1126/sciadv.1600871, 2017.
Riahi, K., Rao, S., Krey, V., Cho, C., Chirkov, V., Fischer, G., Kindermann, G., Nakicenovic, N. and Rafaj, P.: RCP 8.5-A scenario of comparatively high greenhouse gas emissions, Clim. Change, 109(1), 33–57, doi:10.1007/s10584-011-0149-y, 2011.
Segu, P. Q.: Comparison of three downscaling methods in simulating the impact of climate change on the hydrology of Mediterranean basins, J. Hydrol., 383, 111–124, 2010.
Sibson, R: A brief description of natural neighbour interpolation. Interpreting multivariate data, 1981.
Sperber, K. R., Annamalai, H., Kang, I. S., Kitoh, A., Moise, A., Turner, A., Wang, B. and Zhou, T.: The Asian summer monsoon: An intercomparison of CMIP5 vs. CMIP3 simulations of the late 20th century, Clim. Dyn., 41(9–10), 2711–2744, doi:10.1007/s00382-012-1607-6, 2013.
Tan, Ruizhi: A Study on the Regional Energetics during Break, Transitional and Active Periods of the Southwest Monsoon in South East Asia, SCIENTIA ATMOSPHERICA SINICA, 1994.
Taylor, K. E., Stouffer, R. J. and Meehl, G. A.: An overview of CMIP5 and the experiment desing. American Meteorological Society, Bulletim Am. Meteorol. Soc., 93, 485–498, doi:10.1175/BAMS-D-11-00094.1, 2012.
Teutschbein, C. and Seibert, J.: Bias correction of regional climate model simulations for hydrological climate-change impact studies: Review and evaluation of different methods, J. Hydrol., 456–457, 12–29, doi:10.1016/j.jhydrol.2012.05.052, 2012.
Teutschbein, C. and Seibert, J.: Is bias correction of regional climate model (RCM) simulations possible for non-stationary conditions, Hydrol. Earth Syst. Sci., 17(12), 5061–5077, doi:10.5194/hess-17-5061-2013, 2013.
Toggweiler, J. and Key, R.: Ocean circulation: Thermohaline circulation, Encycl. Atmos. Sci., 4, 1549–1555., doi:10.1002/joc, 2001.
Trenberth K E.: Changes in precipitation with climate change, Clim. Res., 47(1–2), 123–138, 2011.

Wang H, Zhao G, Peng J, et al.: Precipitation characteristics over five major river systems of Poyang drainage areas in recent 50 years. Resources and Environment in the Yangtze Basin, 7, 615-619, 2009.
Wang, J., Hong, Y., Li, L., Gourley, J. J., Khan, S. I., Yilmaz, K. K., Adler, R. F., Policelli, F. S., Habib, S., Irwn, D., Limaye, A. S., Korme, T. and Okello, L.: The coupled routing and excess storage (CREST) distributed hydrological model, Hydrol. Sci. J., 56(1), 84–98, doi:10.1080/02626667.2010.543087, 2011.
Weisheimer, R. M. A. L. A. and Gutiérrez, J. M.: Can bias correction and statistical downscaling methods improve the skill of seasonal precipitation forecasts ?, Clim. Dyn., 50(3), 1161–1176, doi:10.1007/s00382-017-3668-z, 2018.
Wilby, R. and Dawson, C. W.: SDSM 4.2-A decision support tool for the assessment of regional climate change impacts, 94, 2007.
Wilks, D. S.: Use of stochastic weather generators for precipitation downscaling, Wiley Interdiscip. Rev. Clim. Chang., 1(6), 898–907, doi:10.1002/wcc.85, 2010.
WU, G., LIU, Y., ZHAO, X., & YE, C.: Spatio-temporal variations of evapotranspiration in Poyang Lake Basin using MOD16 products, Geographical Research, 32(4), 617-627, 2013.
Wu, J., Zha, J. and Zhao, D.: Evaluating the effects of land use and cover change on the decrease of surface wind speed over China in recent 30 years using a statistical downscaling method, Clim. Dyn., 48(1–2), 131–149, doi:10.1007/s00382-016-3065-z, 2017.
Wu, Q., Nie, Q., Zhou, R.: Analysis of wind energy resources reserves and characteristics in mountain area of Jiangxi province, Journal of Natural Resources, 28(9), 1605-1614, doi: 10.11849/zrzyxb.2013.09.015, 2013.
Xu, C. Y.: From GCMs to river flow: A review of downscaling methods and hydrologic modelling approaches, Prog. Phys. Geogr., 23(2), 229–249, doi:10.1191/030913399667424608, 1999.
Ye, X., Zhang, Q., Bai, L. and Hu, Q.: A modeling study of catchment discharge to Poyang Lake under future climate in China, Quat. Int., 244(2), 221–229, doi:10.1016/j.quaint.2010.07.004, 2011.
Yuan, W.: Diurnal cycles of precipitation over subtropical China in IPCC AR5 AMIP simulations, Adv. Atmos. Sci., 30(6), 1679–1694, doi:10.1007/s00376-013-2250-9, 2013.
Yukimoto, S., Adachi, Y., Hosaka, M., et al.: A New Global Climate Model of the Meteorological Research Institute: MRI-CGCM3-Model Description and Basic Performance, J. Meteorol. Soc. Japan, 90A, 23–64, doi:10.2151/jmsj.2012-A02, 2012.
Zhan, M., Yin, J. and Zhang, Y.: Analysis on characteristic of precipitation in Poyang Lake Basin from 1959 to 2008, Procedia Environ. Sci., 10, 1526–1533, doi:10.1016/j.proenv.2011.09.243, 2011.
Zhang, L., Lu, J., Chen, X., Liang, D., Fu, X., Sauvage, S. and Perez, J. M. S.: Stream flow simulation and verification in ungauged zones by coupling hydrological and hydrodynamic models: A case study of the Poyang Lake ungauged zone, Hydrol. Earth Syst. Sci., 21(11), 5847–5861, doi:10.5194/hess-21-5847-2017, 2017.
Zhang, Q., Ye, X. chun, Werner, A. D., Li, Y. liang, Yao, J., Li, X. hu and Xu, C. yu: An investigation of enhanced recessions in Poyang Lake: Comparison of Yangtze River and local catchment impacts, J. Hydrol., 517, 425–434, doi:10.1016/j.jhydrol.2014.05.051, 2014.
Zhang, X., Wan, H., Zwiers, F. W., Hegerl, G. C. and Min, S. K.: Attributing intensification of precipitation extremes to human influence, Geophys. Res. Lett., 40(19), 5252–5257, doi:10.1002/grl.51010, 2013.
Zhao, Y., Zhu, J. and Xu, Y.: Establishment and assessment of the grid precipitation datasets in China for recent 50 years, J. Meteorol. Sci., 34(4), 4–10, 2014.
Zorita, E. and Von Storch, H.: The analog method as a simple statistical downscaling technique: Comparison with more complicated methods, J. Clim., 12, 2474–2489, doi:10.1175/1520-0442(1999)012<2474:TAMAAS>2.0.CO;2, 1999.

Figures

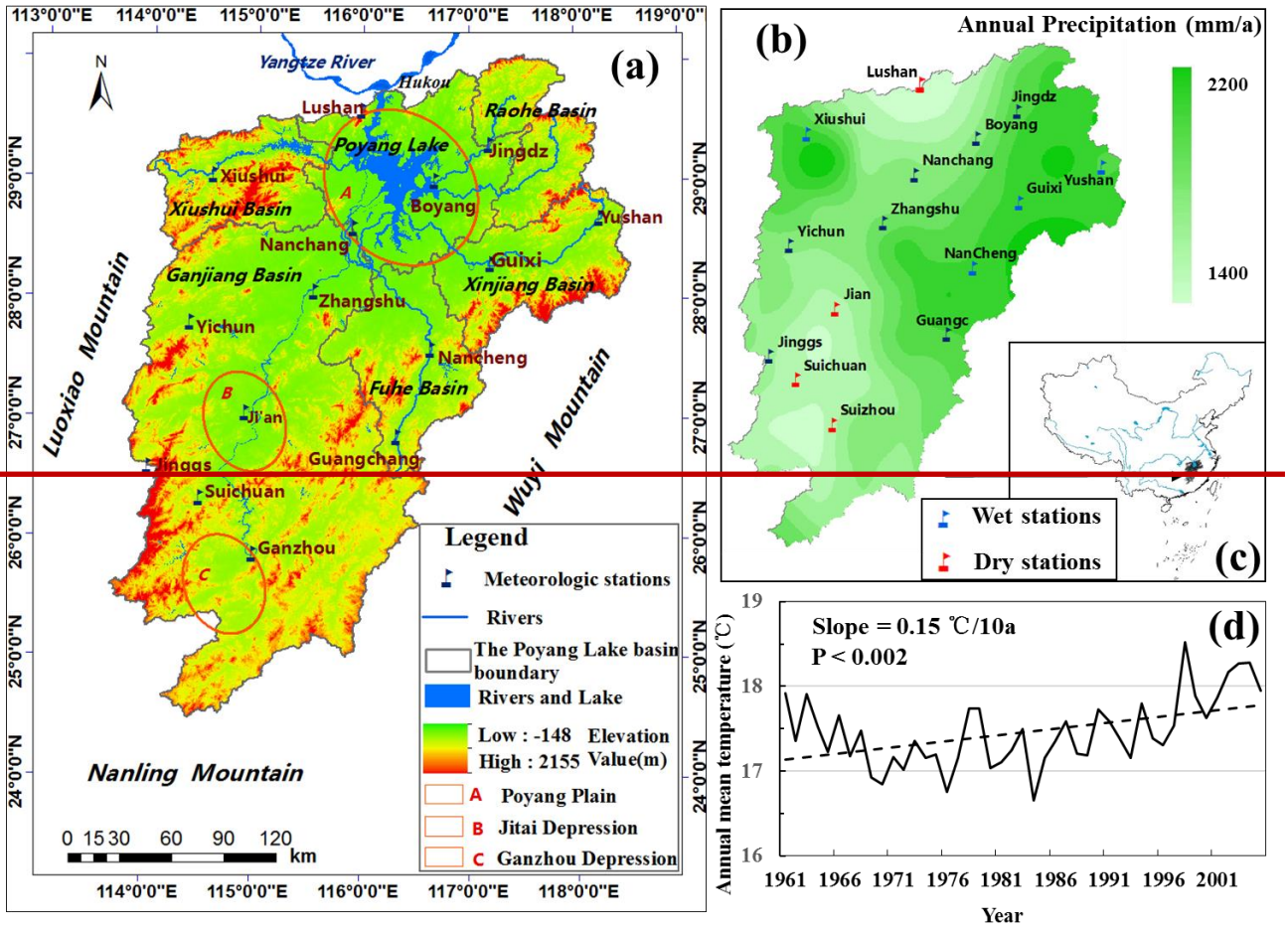
(a)
Yangtze River
Hukou
Lushan
Raohe Basin
Poyang Lake
Jingdz
Xiushui
Xiushui Basin
A
Boyang
Yushan
Nanchang
Guixi
Ganjiang Basin
Xinjiang Basin
Zhangshu
Yichun
Nancheng
Fuhe Basin
B
Ji'an
Luoxiao Mountain
Wuyi Mountain
Jinggs
Guangchang
Suichuan
Ganzhou
C
Nanling Mountain
Legend
Meteorologic stations
Rivers
The Poyang Lake basin boundary
Rivers and Lake
Low : -148 Elevation
High : 2155 Value(m)
A Poyang Plain
B Jitai Depression
C Ganzhou Depression
0 15 30 60 90 120 km
N
113°0'0"E
114°0'0"E
115°0'0"E
116°0'0"E
117°0'0"E
118°0'0"E
119°0'0"
29°0'0"N
28°0'0"N
27°0'0"N
26°0'0"N
25°0'0"N
24°0'0"N
(b)
Annual Precipitation (mm/a)
2200
1400
Lushan
Jingdz
Xiushui
Boyang
Nanchang
Guixi
Yushan
Zhangshu
Yichun
NanCheng
Jian
Guangc
Jinggs
Suichuan
Suizhou
Wet stations
Dry stations
(c)
(d)
Slope = 0.15 ℃/10a
P < 0.002
Annual mean temperature (℃)
19
18
17
16
1961
1966
1971
1976
1981
1986
1991
1996
2001
Year

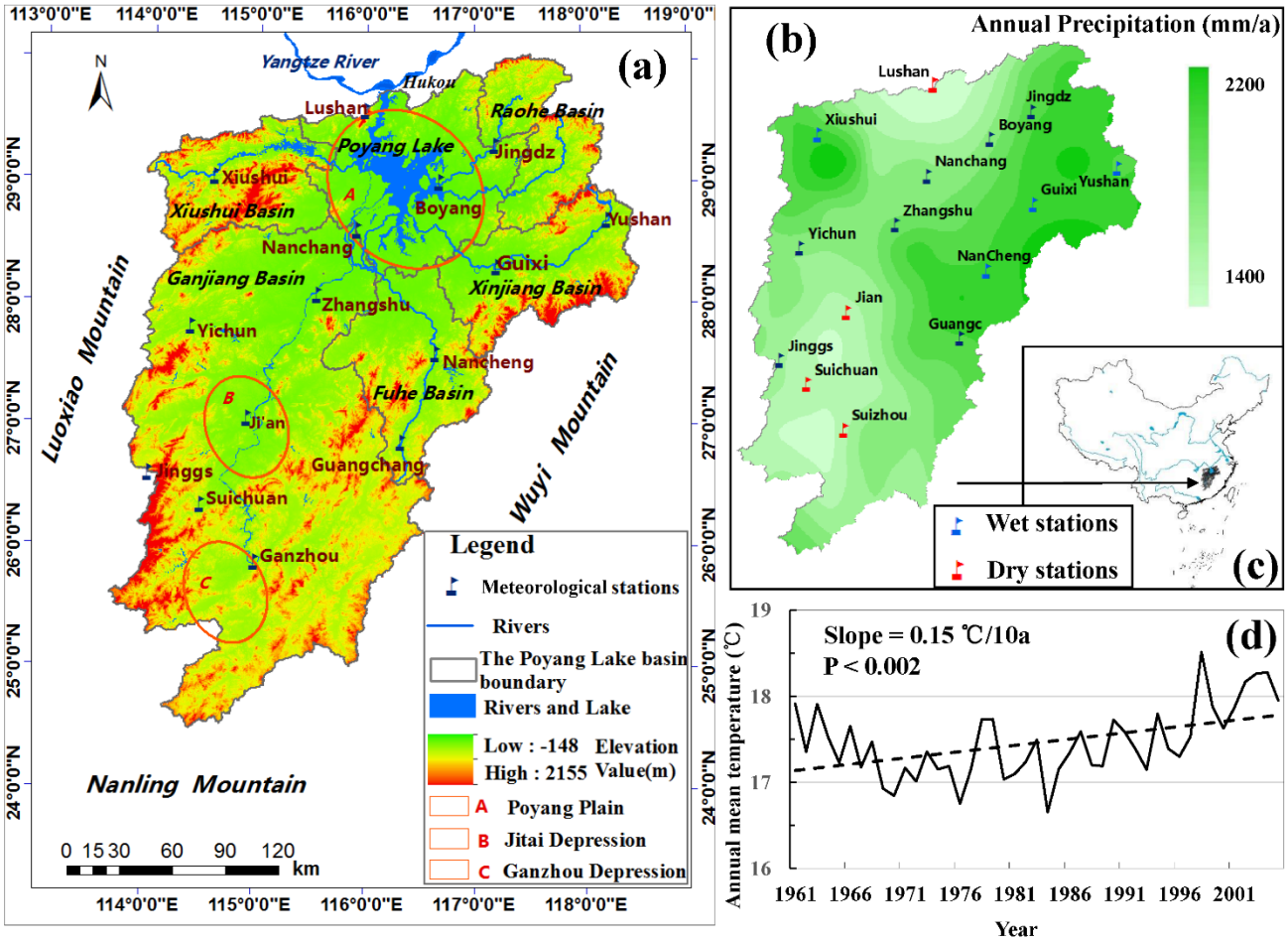

Fig. 1. The topography and landforms (a), precipitation distribution and dry-wet stations (b), temperature change (d) and location of the Poyang Lake Basin (c). We sorted ~~annual total precipitations~~the annually accumulated precipitation of the 15 stations, averaged over time from 1961 to 2005~~, of the 15 stations.~~ The 4 stations with the max or min mean annual precipitations are set as dry or wet stations, respectively.

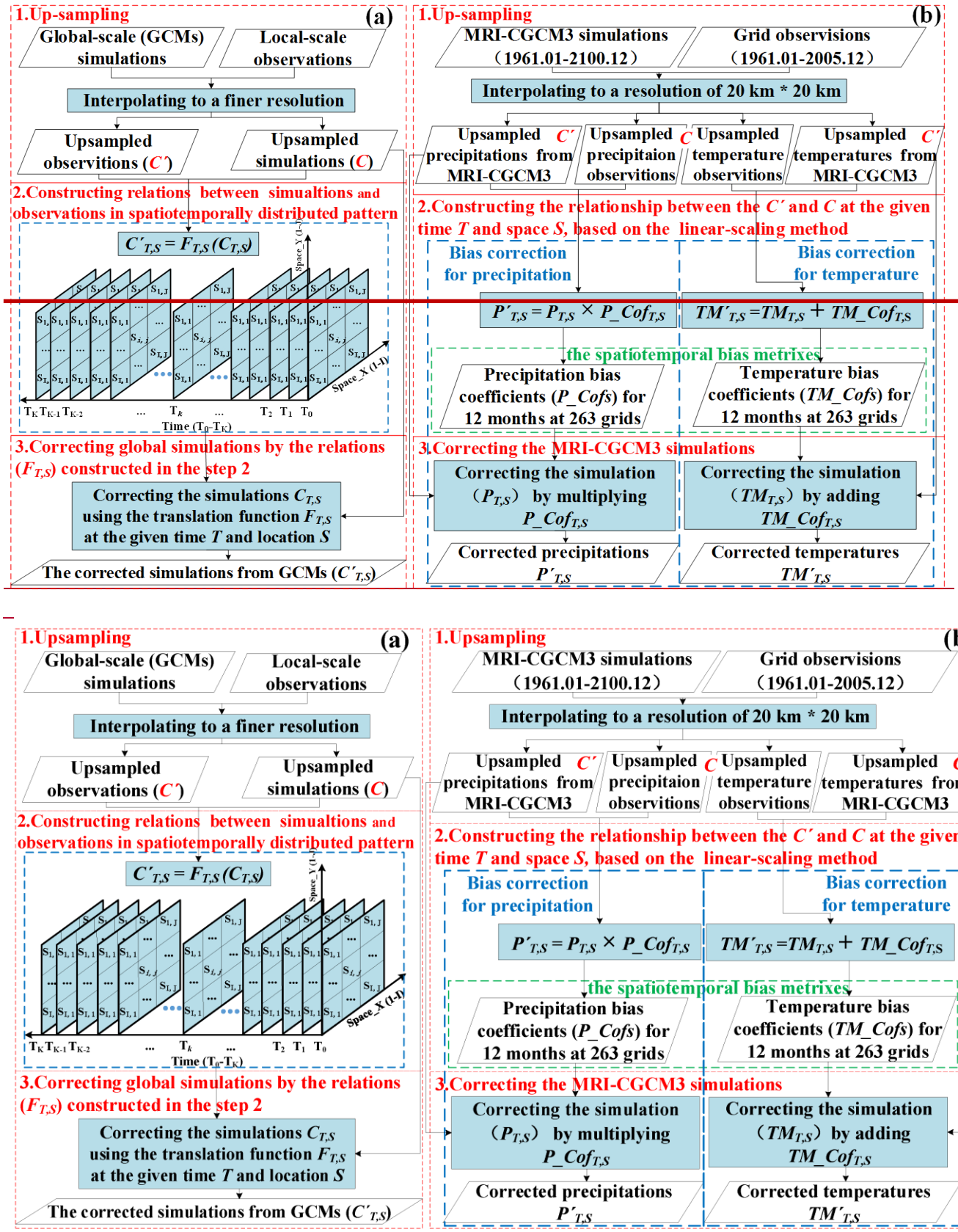

Fig. 2 Conceptual flow chart of the climate projection including ~~up-sampling~~upsampling, relation construction and correction: The common framework of the STDDM (a) and test case base on the linear-scaling algorithm (b). The STDDM was used to ~~projected~~project MRI-CGCM3 simulations from 1998 to 2100.

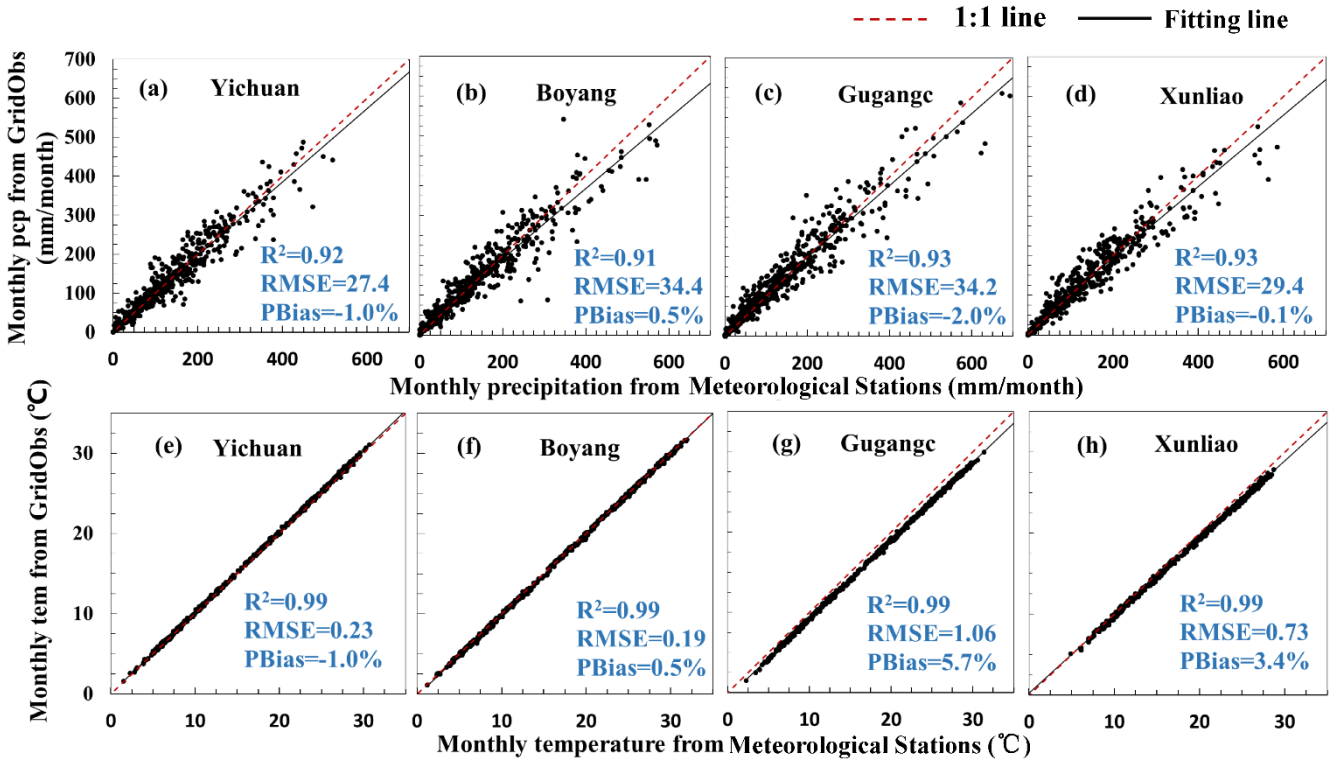

Fig. 3. Validation of gridded meteorological data (GridObs) by using gauging stations observation: Precipitation (pcp; a,b,c and d) and temperature (tem; e,d,f and g) at meteorological station of Jian (a and e), Ganzhou (b and d), Zhangshu (c and f) and Lushan (d and g).

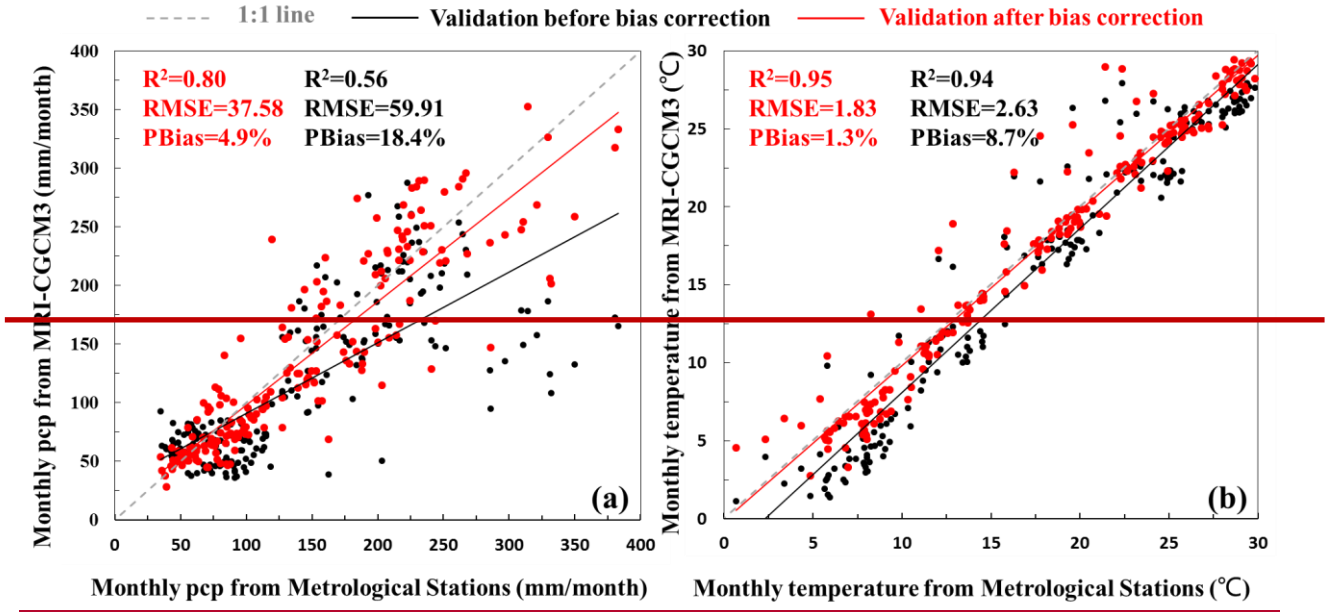

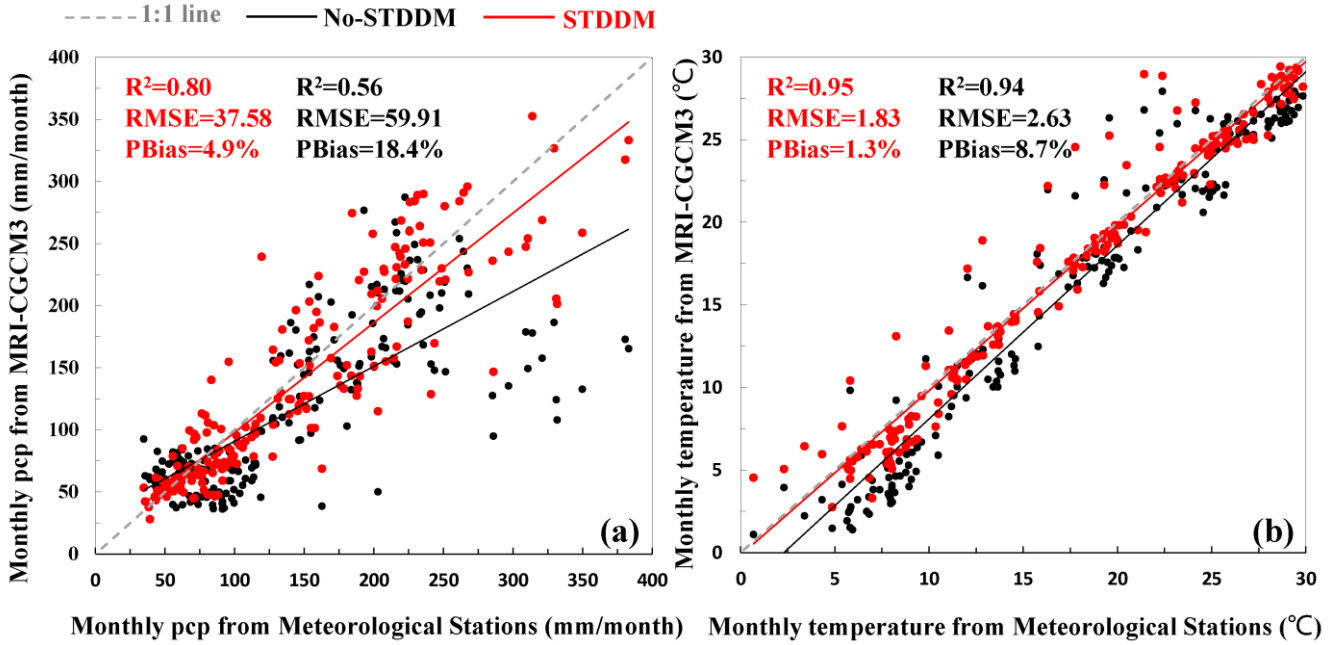

Fig. 4. Validation of the precipitation (pcp) (a) and temperature (b) ~~projection before~~projections by the STDDM (in black) and ~~after~~No-STDDM (in red~~) bias correction.~~). Dots represent the monthly precipitations (or ~~temperature) from January to December,~~temperatures), averaged over 20 years from 1986 to 2005. The dots contain monthly precipitations of the 15 stations. The solid lines represent linear regression which is the best fit ~~though~~through all match-ups of the projections and observations.

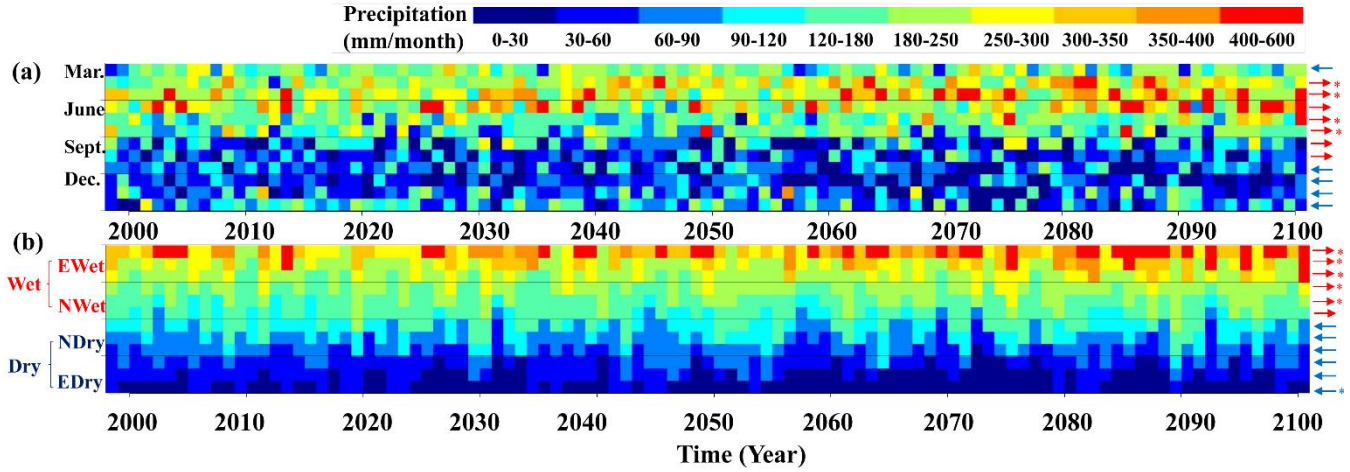

Fig. ~~4~~5. Total variability of monthly precipitation from 1998 to 2100. Each column represents the data ~~of~~for one year and each cell represents an accumulative precipitation of one month. The red ~~and~~ (blue) arrows indicate that the monthly precipitation experienced an increasing ~~or~~ (decreasing ~~trends~~) trend over the 103 years, respectively. The asterisk demonstrates the significant trends with $p<0.05$. (a) Monthly precipitation in month order, referred to Spring (March to May), summer (June to August), autumn (September to November), and winter (December to next February) from top to bottom, respectively. (b) Monthly precipitation, sorted in the descending order for each year, where months are classified as extreme wet (EWet), normal wet (NWet), normal dry (NDry) and extreme dry (Edry) months from up to down. Therein, wet months (Wet) include extreme and normal wet ones while dry months (Dry) include extreme and normal dry ones.

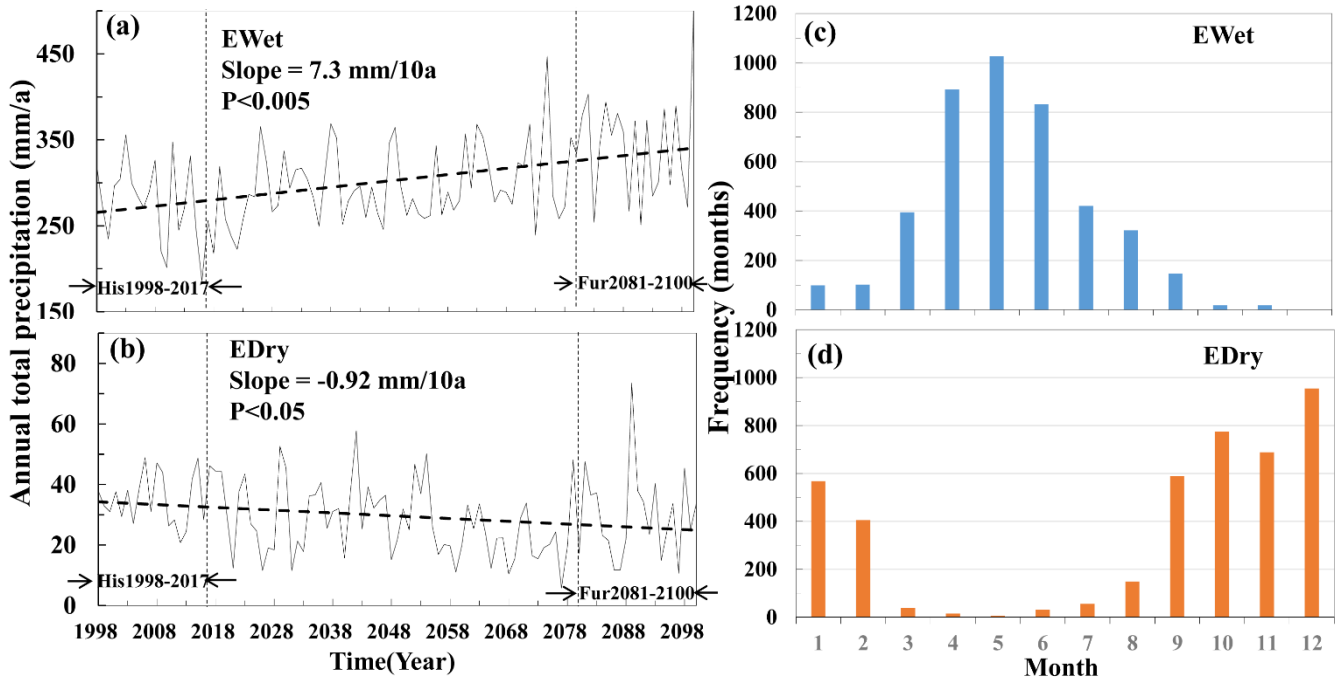

Fig. ~~5~~6. The ~~change~~ trends of changes in monthly precipitations of extreme wet (EWet) (a) and dry (EDry) (b) months from 1998 to 2100. The ~~far~~further future period from 2081 to 2100 (Fur2081-2100) and baseline period from 1998 to 2017 (His1998-2017) are indicated by arrows. Frequencies of the ~~Months~~months in extreme wet (c) or dry (d) months are calculated during the period from 1998 to 2100.

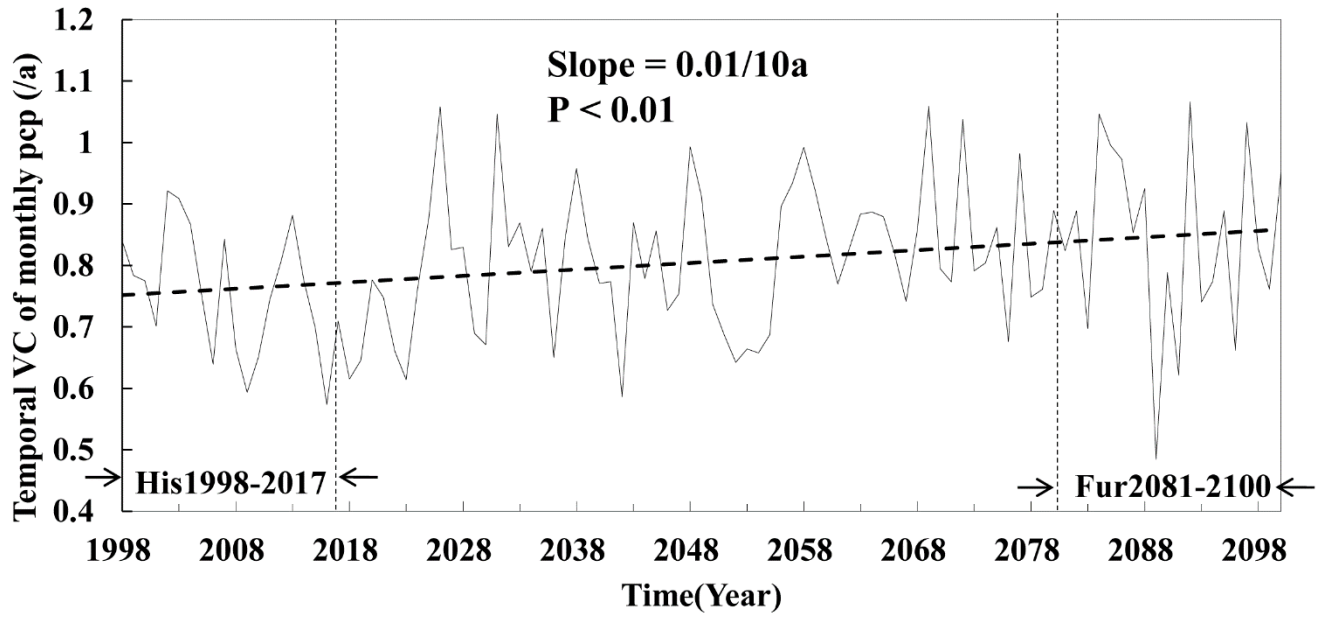

Fig. ~~6~~7. The temporal variation coefficients of the extreme month precipitations for each year over 1988 to 2100. The extreme months are composed of the extreme wet and dry months. The far future period from 2081 to 2100 (Fur2081-2100) and baseline period from 1998 to 2017 (His1998-2017) are indicated by arrows.

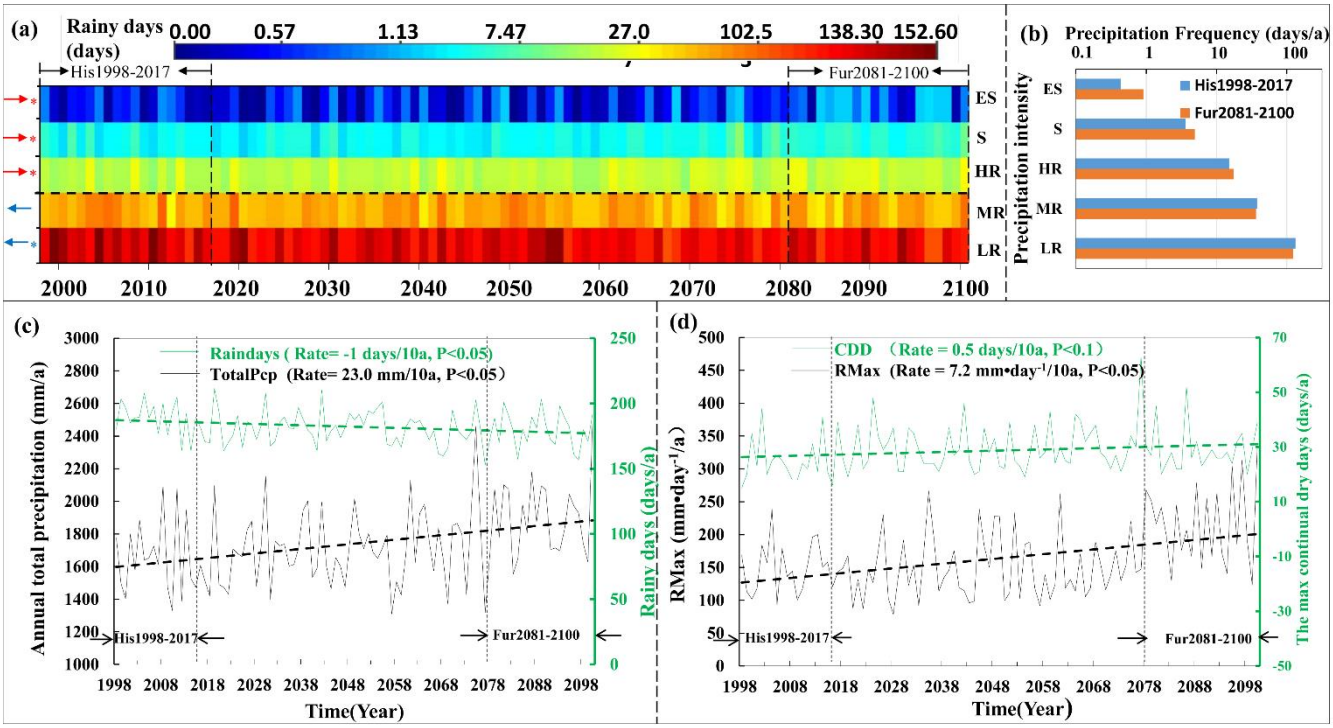

Fig. ~~7~~8. The changes ~~of~~in daily precipitation intensities and frequencies. (a) Precipitation intensities and frequencies for each year over 1998 to 2100, where each column represents a year and each row indicates a precipitation intensity. Daily precipitation intensities are categorized to 5 classes, Light Rain (LR), Median Rain (MR), Heavy Rain (HR), Rainstorm (S), and Extreme Rainstorm (ES) with daily precipitation ~~in~~of 0.1-10, 10-25, 25-50, 50-100 and >100 mm/day, respectively. The moderate rain includes LR and MR while the extreme rain is composed of HR, S, and ES. The cell represents an annual frequency of one precipitation intensity, with a unit of days. The red ~~or~~ (blue) arrows indicate that annual frequency of the precipitation intensity experienced an increasing ~~or~~ (decreasing) trends over the 103 years (from 1998 to 2100), respectively. The asterisk represents the significant trends with $p<0.05$. The far future period from 2081 to 2100 (Fur2081-2100) and baseline period from 1998 to 2017 (His1998-2017) are indicated by arrows. (b) Precipitation frequencies of LR, MR, HR, S, and ES for Fur2081-2100 and His1998-2017, respectively. (c) The change of the long-term data for annual total precipitation (totalPcp) and total rainy days~~-~~ (Raindays). (d) The change of the long-term data for annual max daily precipitation (RMax) and annual max continuous dry days (CCD).

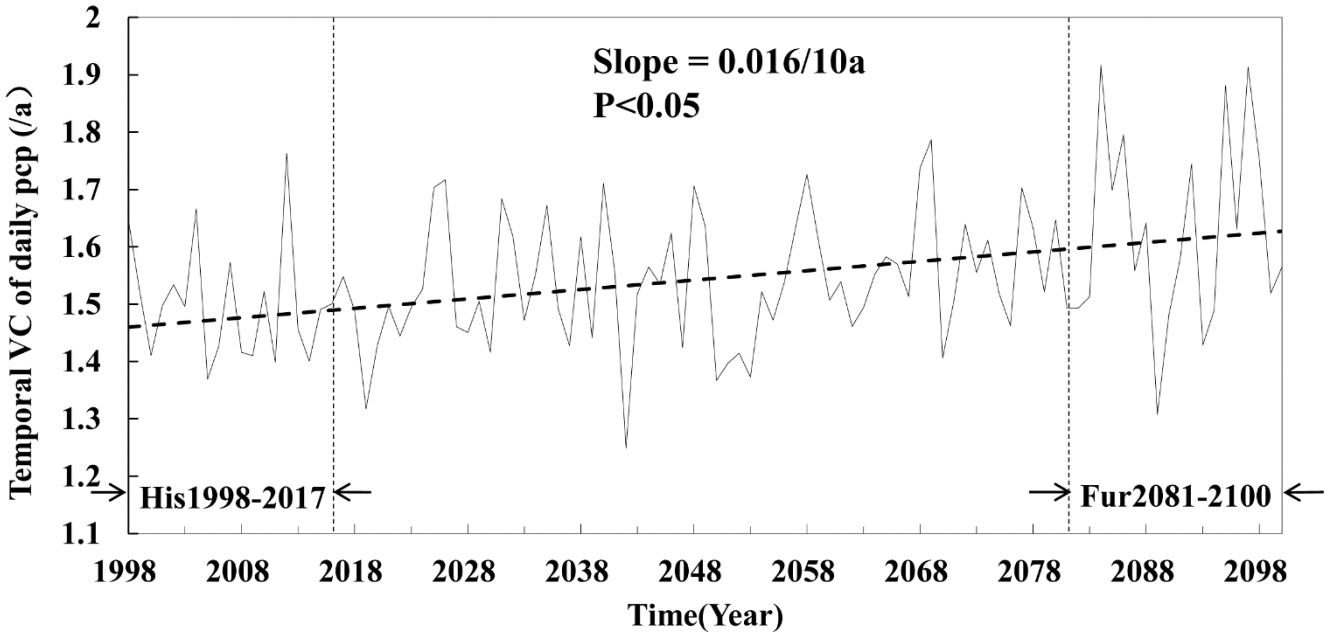

Fig. ~~8~~9. The temporal variation coefficient of daily precipitations for each year over 1988 to 2100. The far future period from 2081 to 2100 (Fur2081-2100) and baseline period from 1998 to 2017 (His1998-2017) are indicated by arrows.

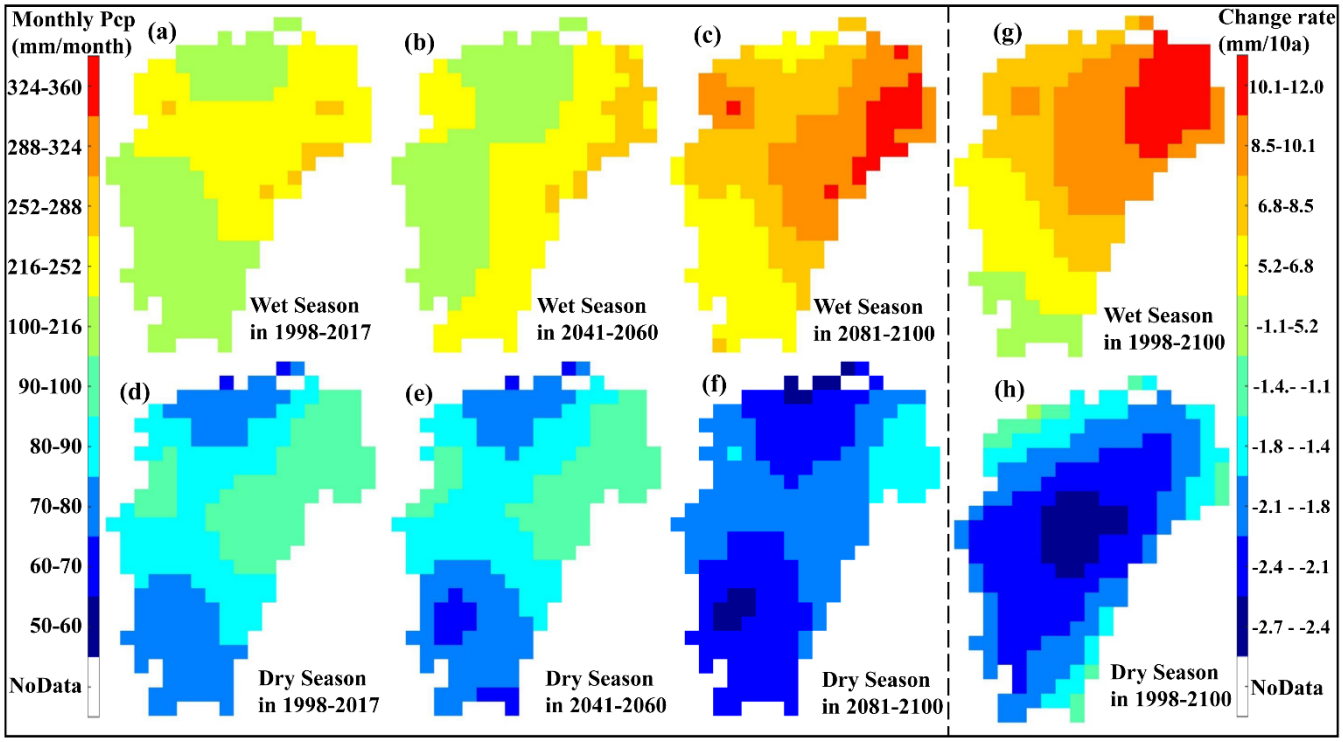

Fig. ~~9~~10. The precipitation changes in the spatial pattern during the period from 1998 to 2100: average monthly precipitations of the wet season (April to July) during the ~~historical~~ period from 1998 to 2017 (a), 2041 to 2060 (b), and 2081 to 2100 (c); average monthly precipitations of the ~~wet~~dry season (~~April~~December to ~~July~~next February) during the historical period from 1998 to 2017 (d), 2041 to 2060 (e), and 2081 to 2100 (f); change rate of monthly precipitation in wet (g) and dry (h) season from 1998 to 2100. As floods and droughts occur more frequently in extreme months, the precipitation in the analysis considered only the extreme wet (April-July) and dry (September-February) months (Fig. 5c and d). Besides, precipitation is dominated by southeast summer monsoon, which brings water vapor from the sea. The summer monsoon is frequent from the end of spring and stat of autumn, covering the wet months April to July. However, though as dry months, the autumn period from

September to November is affected by southeast summer monsoon (Tan et al., 1994) slightly because autumns are the transpiration periods of summer to winter. Therefore, winter (December-February) was represented as the dry season with poor rain; while April-July was represented as the wet season with abundant rain.

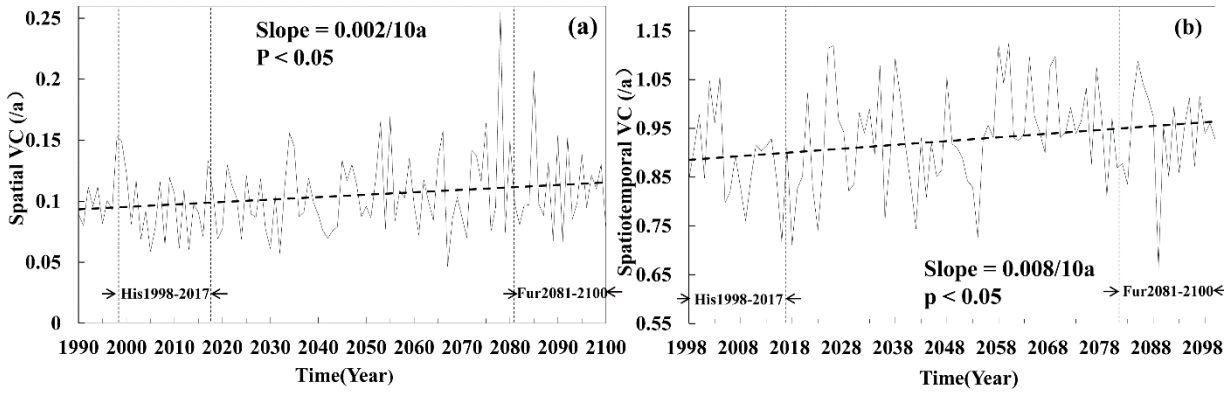

Fig. ~~10~~11. The spatial (a) and spatiotemporal (b) variation coefficient for each year over 1988 to 2100. The ~~far~~further future period from 2081 to 2100 (Fur2081-2100) and baseline period from 1998 to 2017 (His1998-2017) are indicated by arrows.

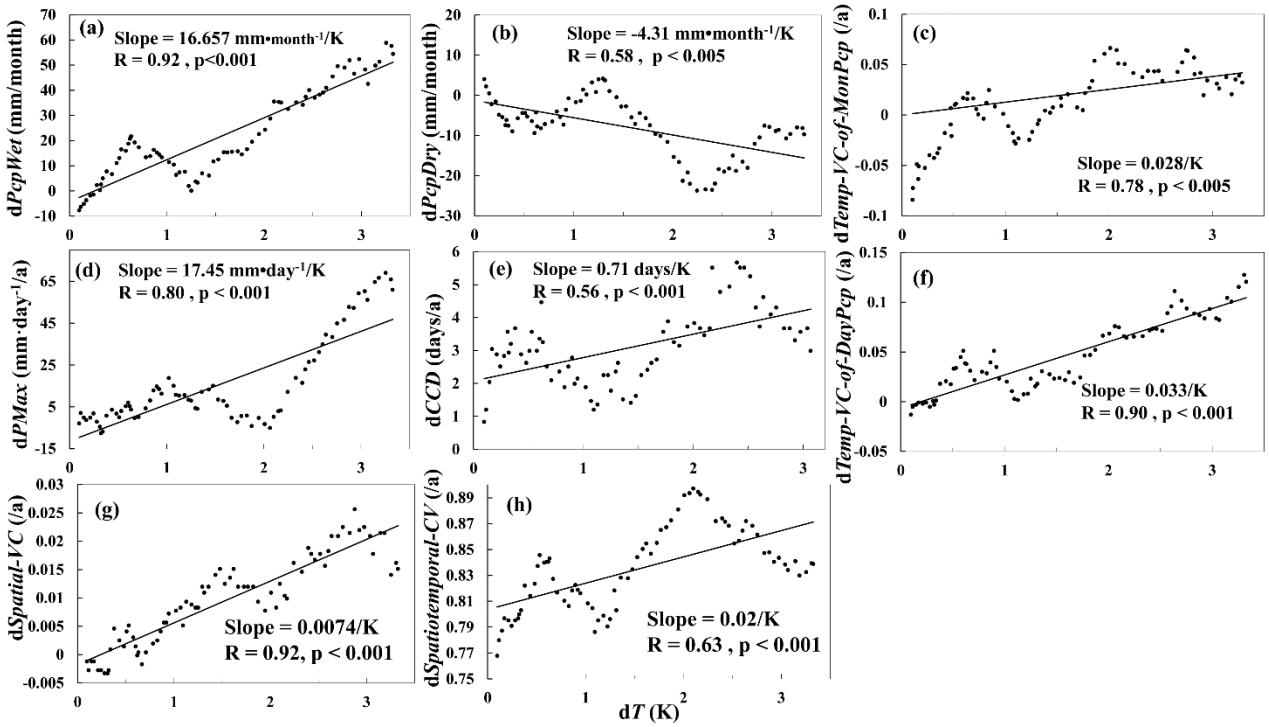

Fig. ~~11~~12. The relationship between the precipitation ~~indexes~~index changes (d*PcpIndex*) and the temperature ~~changes~~increment (d*T*). The precipitation indexes include annual precipitation in the wet season (PcpWet) (a), annual precipitation in the dry season (PcpDry) (b), temporal variance coefficient of monthly precipitations (Temp-VC-of-MonPcp) (c), annual max daily precipitation (PMax) (d), annual max ~~continual~~continuous dry days (CCD) (e), temporal variance coefficient of daily precipitations (Temp-VC-of-DayPcp) (f), spatial variance coefficient (Spatial-VC) (g), and spatiotemporal variance coefficient (Spatiotemporal-VC) (h). All the precipitation

index changes show significant correlations with temperature ~~increases.~~increment.